

# ***EUDP Project Offshore Wind Turbine Reliability through complete Loads Measurements***

---

Anand Natarajan, Allan Vesth, Christina Koukoura, Steen Sørensen, Ginka Yordanova, Thomas Buhl  
Kenneth Thomsen

DTU Wind Energy

Thomas Krogh, Ole Jesper Dahl Kristensen  
DONG Energy

Jesper Stærdahl  
Siemens Wind Power

**Project Final Report**

**Project no 64010 -0123**

**Funded by the Energy Technology Development and Demonstration Programme (EUDP)**

<b>Project title</b>	Offshore Wind Turbine Reliability through complete Loads Measurements
<b>Project identification (program abbrev. and file)</b>	J.nr. 64010-0123
<b>Name of the programme which has funded the project</b>	Energiteknologisk udvikling og demonstration (EUDP)
<b>Project managing company/institution (name and address)</b>	DTU Vindenergi, Risø Campus, Frederiksborgvej 399, 4000 Roskilde
<b>Project partners</b>	Siemens, DONG
<b>CVR (central business register)</b>	30060946
<b>Date for submission</b>	Jul 15, 2015

## Table of Contents

1.0 Short description of project objective and results .....	4
1.1 Executive summary .....	4
1.2 Project objectives .....	4
Project results and dissemination of results .....	5
2.0 Measurement Wind Turbine Technical Description .....	5
3.0 Wind Farm and Environment Description (Thomas Krogh, DONG).....	6
Site conditions.....	8
Wind Conditions .....	8
Oceanographic conditions.....	8
4.0 Turbine Measurement System and its Calibration.....	10
Measurement system:.....	10
Hub/Rotor Load Sensors .....	10
Nacelle .....	12
Transition piece.....	17
Calibrations.....	19
5.0 Description of Database of Measurements and Access .....	21
6.0 Wind and SCADA Measurements .....	48
6.1 Cup anemometers and nacelle-based lidar.....	48
6.2 SCADA measurements .....	50
7.0 Validation of Environmental Models and Load Simulations with Measurements .....	52
Wind Turbine Model set-up.....	54
Nacelle LIDAR.....	55
Wave Measurement Analysis.....	56
Validations of Loads on the Foundation .....	60
8.0 Evaluation of Support Structure Damping.....	65
9.0 Key Factors affecting Support Structure Cost .....	68
10.0 Recommendations to IEC Standards.....	73
11.0 Summary of Results and Dissemination (Anand).....	74
References, List of Publications, Reports (Publications made from project results are in bold).....	75

## **1.0 Short description of project objective and results**

A 3.6MW Siemens offshore wind turbine was fully instrumented for loads measurements, along with foundation strain gauges, a wave buoy and nacelle LIDAR based wind measurements. Further online SCADA measurements of the turbine operation and performance along with surrounding turbines were collected. The measurements were made over a 3.5 year period from 2011-2015 and formed the basis for a comprehensive validation of aeroelastic loads simulations and estimation of damping of offshore support structures. The results of these studies have been published in 2 journal papers, a Ph.D. thesis and 3 conference publications. The database of loads, performance and environmental conditions is maintained at DTU wind energy.

### **1.1 Executive summary**

Load simulations on the substructure and blade are validated by comparing the results from the aero-hydro-servo-elastic design tool HAWC2 with measurements from the instrumented wind turbine. The damping of the support structure has been quantified using measured tower accelerations and this is used as an input for extreme loads and fatigue loads analysis. The wind farm wake effects on the monopile fatigue loads is also examined and compared with load measurements. Potential recommendations for the design of offshore wind turbines are detailed and explained.

### **1.2 Project objectives**

The specific objectives of the project were

1. Experimental evidence of load magnitudes on modern offshore wind turbines to support software model development. The measurements will be specifically designed to quantify loads on main components of the wind turbine under various operational conditions
2. Investigate foundation and tower dynamics, and by means of the measurements and modeling work, predict the structural loads and response of very large offshore wind turbines substructures.
3. Investigate and model specific important design drivers such as damping of support structures
4. Evaluate wake effects in very large wind farms such as the Walney wind farm and its impact on fatigue loads

## Project results and dissemination of results

### 2.0 Measurement Wind Turbine Technical Description

The instrumented wind turbine is a Siemens 3.6 MW 107m rotor diameter turbine which is variable speed pitch controlled and is mounted on a monopile foundation. It has a hub height of 83.6m above the sea surface. The turbine has a cut-out mean wind speed of 25m/s and does not have storm control. The turbine is installed in the Walney wind farm phase 1 area and is denoted as turbine number D01.

The wind turbine operates automatically, self-starting when the wind reaches an average speed between 3–5 m/s. The power output increases with the wind speed until the wind reaches 13–14 m/s. At that point, the power is regulated at rated power by pitching the blades. If the average wind speed exceeds the maximum operational limit of 25 m/s, the turbine is shut down by feathering of the blades to near 85 degs. The turbine has a planetary 3 stage gearbox with a gear ratio of 119. The rated wind speed of the turbine from which full power is obtained is near 13m/s.



Figure 2.1: Figure depicting wind turbines on the Walney wind farm

### 3.0 Wind Farm and Environment Description

The Walney Offshore Windfarm (WOW) is located in the east Irish sea approximately 15km west of Barrow-in-Furness. The wind farm was built in two phases. Walney 1 which consists of 51 Siemens SWT-3.6-107 turbines had first power in January 2011 and Walney 2 which consists of 51 Siemens SWT-3.6-120 turbines was finalised in April 2012.

Main data for the wind farm are shown in the table below

Total capacity	367.2MW
Distance from shore	14.4 - 25.8 km
Distance between wind turbines	749 - 958 m
Wind farm area	73 km <sup>2</sup>

The test turbine WOW-D01 is located in the south end of the Walney 1 wind farm as shown on the map below.

The West of Duddon Sands wind farm which is located just south of WOW started installation in the fall of 2013 and was fully commissioned in October 2014.

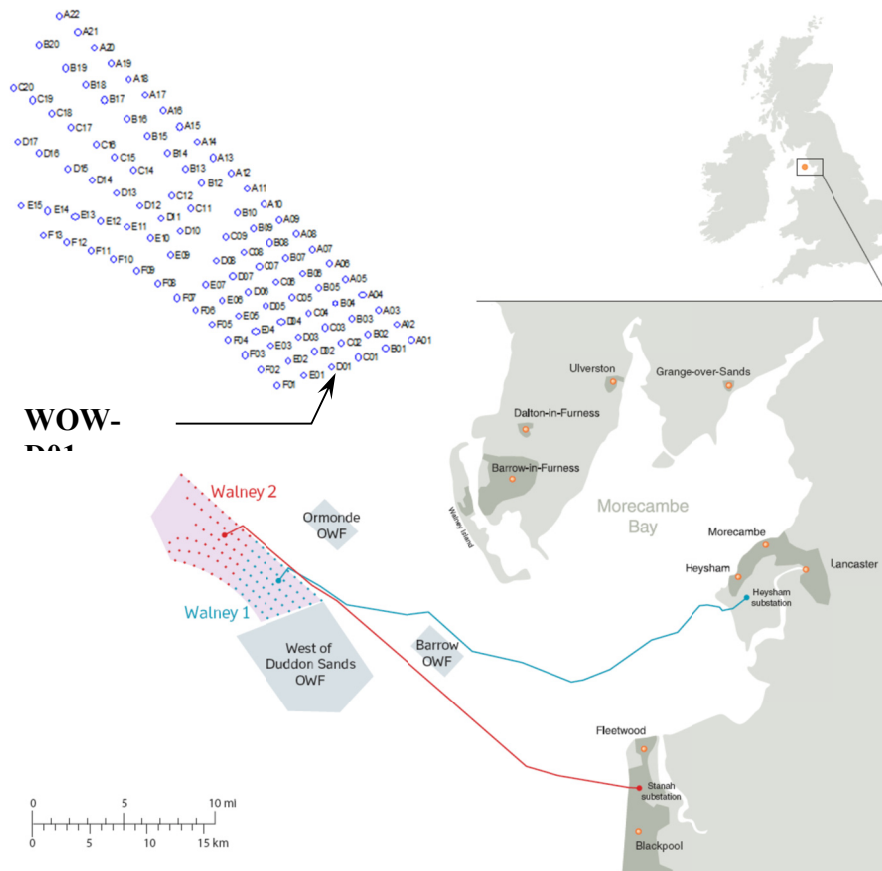


Figure 3.1. Map of the Walney Offshore Windfarm.

The coordinates for the WOW-D01 turbine is in UTM30N, Easting 467.970 and Northing 5.986.041. Further the WOW-D01 has the following main data:

Wind Turbine Generator	Siemens 3.6-107
Foundation type	Monopile
Nominal power	3600 kW
Rotor diameter	107 m
Hub height above LAT	83.60 m
Tower/foundation interface level above LAT	21.85m
Cut-in wind speed	4 m/s
Full power output from	14 m/s
Cut-out wind speed	25 m/s
Weight, blade, each	18 tonne
Weight, nacelle	150 tonne
Weight, rotor	50 tonne
Weight, tower	260 tonne

Total weight per wind turbine	550 tonne
Lowest Astronomical Tide (LAT)	21.0 m
Mean Sea Level (MSL)	LAT + 4.3 m
Highest Astronomical Tide (HAT)	LAT + 8.9 m

## Site conditions

### Wind Conditions

The wind conditions for WOW have been collected from a nearby offshore meteorology mast. The mast is situated approximately 7.1m higher than the wind turbine hub height. A marginal wind speed difference of <1% can be assumed for the two heights. Due to considerations about the overall accuracy of the statistics no changes have been made to adjust for the height difference. The Weibull distribution parameters are listed in the table below.

**Table3.1. Meteorological conditions**

<i>Sector</i>	<i>N</i>	<i>NNE</i>	<i>ENE</i>	<i>E</i>	<i>ESE</i>	<i>SSE</i>	<i>S</i>	<i>SSW</i>	<i>WSW</i>	<i>W</i>	<i>WNW</i>	<i>NNW</i>
<i>Range</i>	345	15	45	75	105	135	165	195	225	255	285	315
	15	45	75	105	135	165	195	225	255	285	315	345
	<i>Weibull distribution parameters for each sector</i>											
<i>A</i>	6.78	7.79	7.92	9.50	9.33	10.96	9.78	11.51	12.32	10.90	9.72	9.25
<i>k</i>	1.79	2.23	2.09	2.64	2.54	2.43	2.18	2.25	2.63	2.20	2.07	2.07
	<i>Wind direction distribution, WI</i>											
	3.4%	5.0%	7.8%	8.8%	7.8%	7.3%	5.4%	9.8%	13.4%	12.6%	12.5%	6.2%

The mean wind for the different directions is given as percentages of the combined weighted mean wind. The resulting average wind speed at hub height is approximately 9.3 m/s

### Oceanographic conditions

The modelled wave climate, as used in the design basis for the wind farm operation range is illustrated in the figure 3.2. As can be seen the wave heights are moderate with the expected significant wave height lower than 3.5m at all operational mean wind speeds.



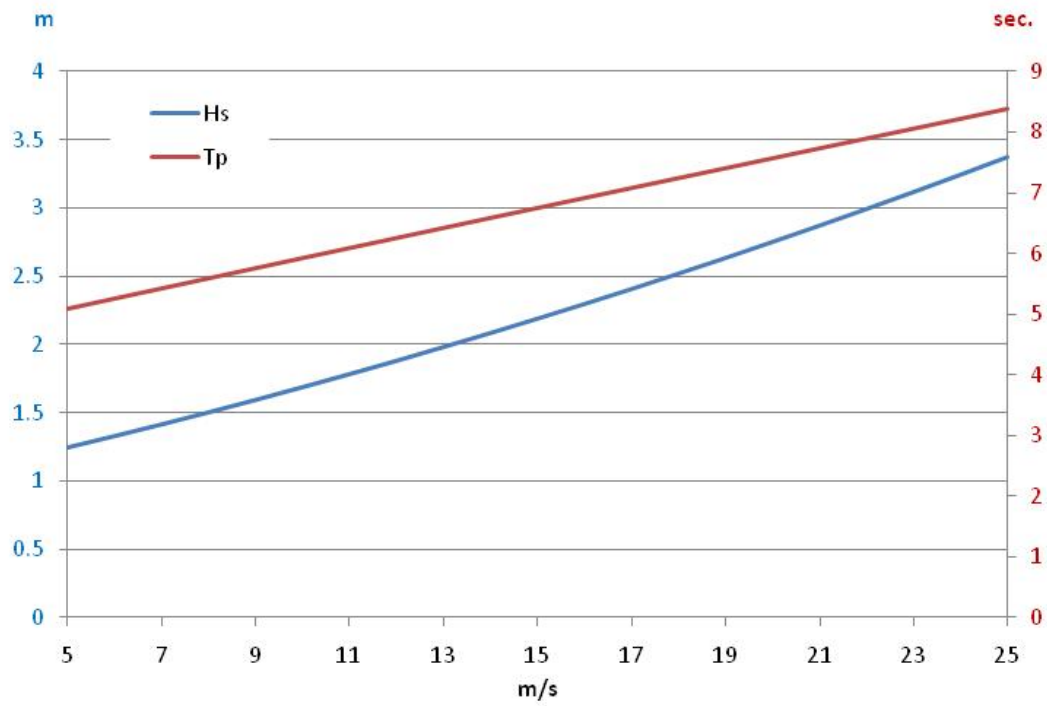


Figure 2.2: Significant wave height  $H_s$  and wave period  $T_p$  dependency on average wind speed.

## 4.0 Turbine Measurement System and its Calibration

### Measurement system:

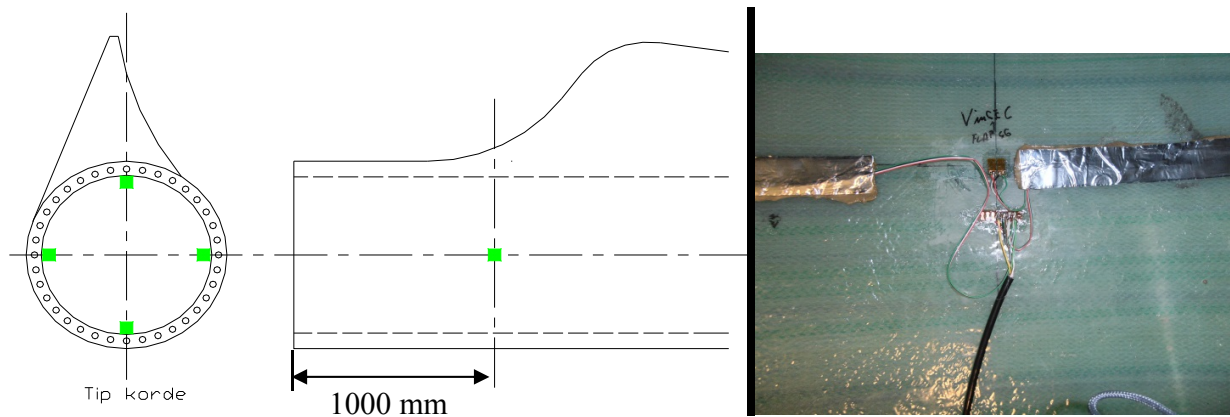
This chapter describes the measurement system as installed on the 3.6 MW offshore wind turbine by DTU. The description includes the various components of the turbine, and the sensor names listed correspond to the sensor names in the database.

The measurement system sampling frequency is 35 Hz and the data was collected in a database together with data from the other measurement systems which are the loads from the monopile and transition piece; SCADA data from the test turbine and surrounding turbines, Nacelle Lidar wind measurements and wave measurements from a Wave buoy

### Hub/Rotor Load Sensors

#### Blades

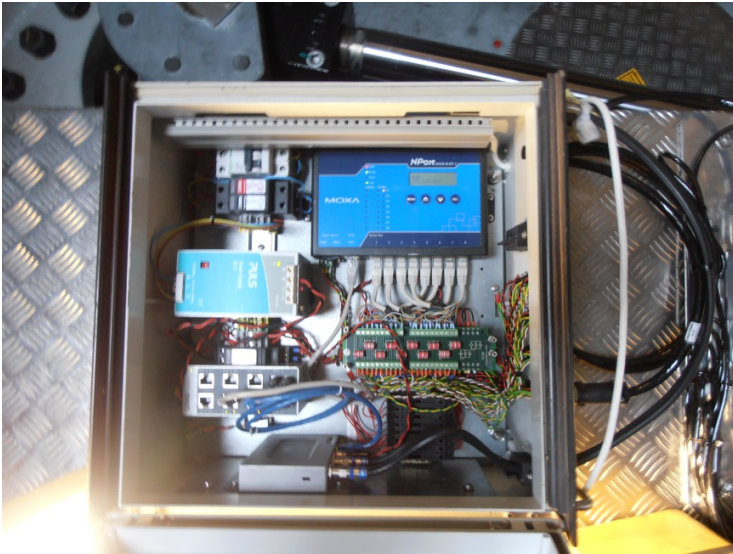
All three blades are equipped with strain gauge bridges measuring bending in edge- and flap-wise direction. The strain gauge bridges are placed 1000mm from the root of the blades.



Sensor Acronyms: **Flap\_b1A, Edge\_b1A, Flap\_b1B, Edge\_b1B, Flap\_b1C, Edge\_b1C**

**Pitch angle, and Yaw direction:**

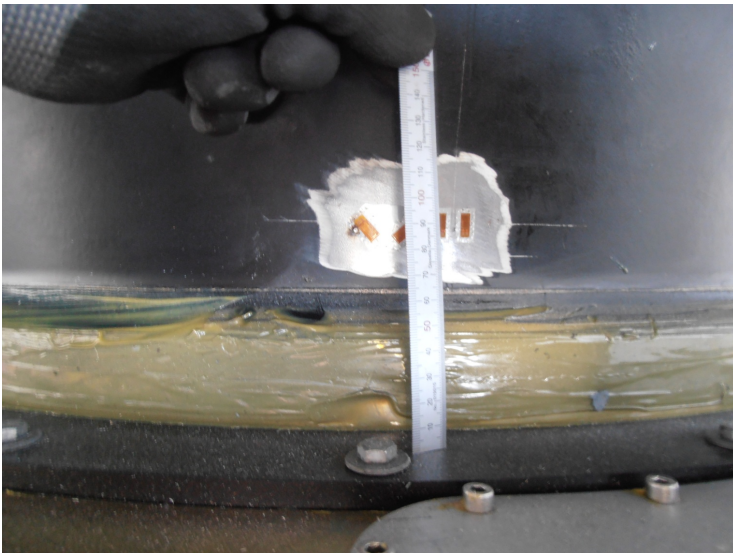
The blade pitch angle signal, Pitch angle reference signal and yaw direction from the turbine controller is delivered from the turbine monitoring system from Siemens and sampled by DTU.



Sensor names: **PosA, PosB, PosC, RefA, RefB, RefC, Yaw.**

**Main shaft:**

The main shaft is equipped with strain gauge bridges measuring bending in 0-180 °, 90-270 ° direction and torsion. The strain gauge bridges are placed 90mm from the main bearing support. The torsion signal is influenced by cross-torque from the bending of the main shaft.

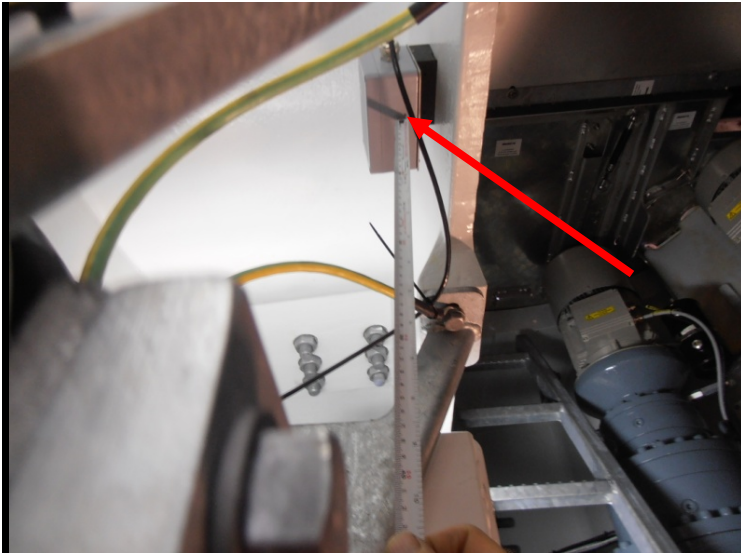


Sensor names: **Shaft\_Torq, Shaft\_0\_180, Shaft\_90\_270.**

## Nacelle

### Acceleration center of nacelle.

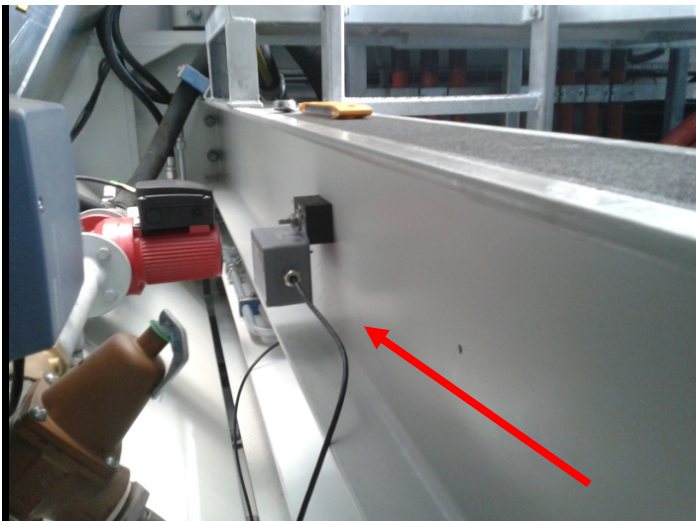
An accelerometer measuring accelerations in three directions is placed on the nacelle frame under the gearbox close to the centerline of the tower (center).



Sensor names: **AccZ\_center**, **AccX\_center**, **AccY\_center**.

### Accelerations Rear of nacelle.

Another accelerometer measuring accelerations in three directions is placed on the nacelle frame at the rear of the nacelle (Rear).



Sensor names: **AccZ\_Rear**, **AccX\_Rear**, **AccY\_Rear**.

### **Rotor position and rpm.**

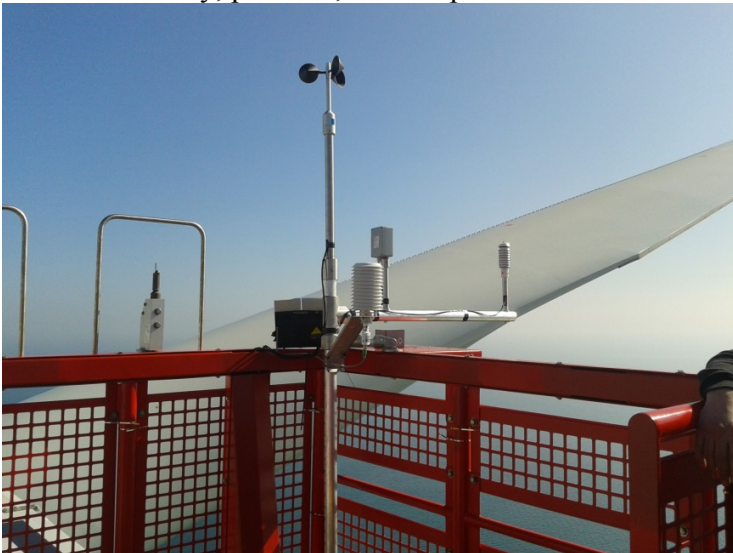
An Inductive Sensor has been installed on the high speed shaft and a reset sensor on the main bearing support. This system delivers the rotor position and rpm for the low- and high speed shaft.



Sensor names: **LS\_Shaft, HS\_Shaft, Rotor\_pos.**

### **Nacelle Wind speed, relative humidity, pressure, and temperature:**

A Thies "First Class" Advanced Cup Anemometer has been installed on top of the nacelle together with relative humidity, pressure, and temperature sensors.



Sensor names: **Wsp\_thies, RH\_Top, Vaisala\_temp\_Top, Press\_top, Tabs\_Top.**



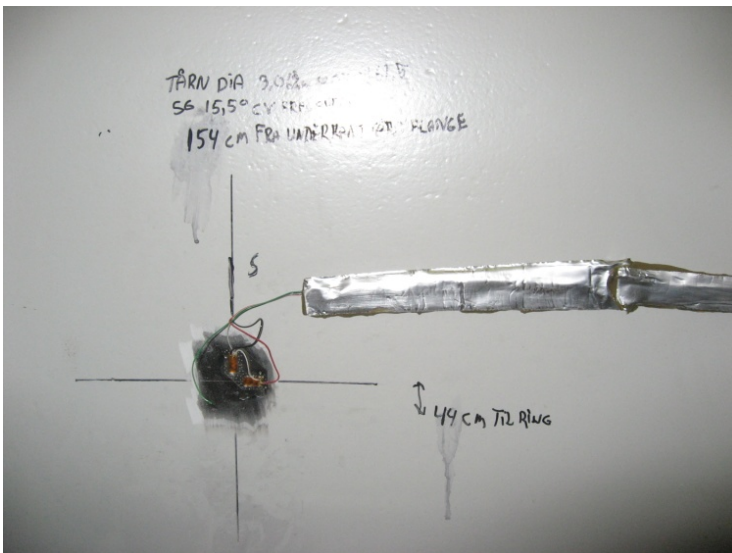
### **Tower:**

The tower is equipped with:

- Strain gauge bridges measuring bending in North / South and East / West directions at three heights.
- One strain gauge bridge measuring tower torsion placed on the tower top.
- Two accelerometers measuring accelerations in three directions were placed at the tower middle and the tower bottom.

### **Tower top**

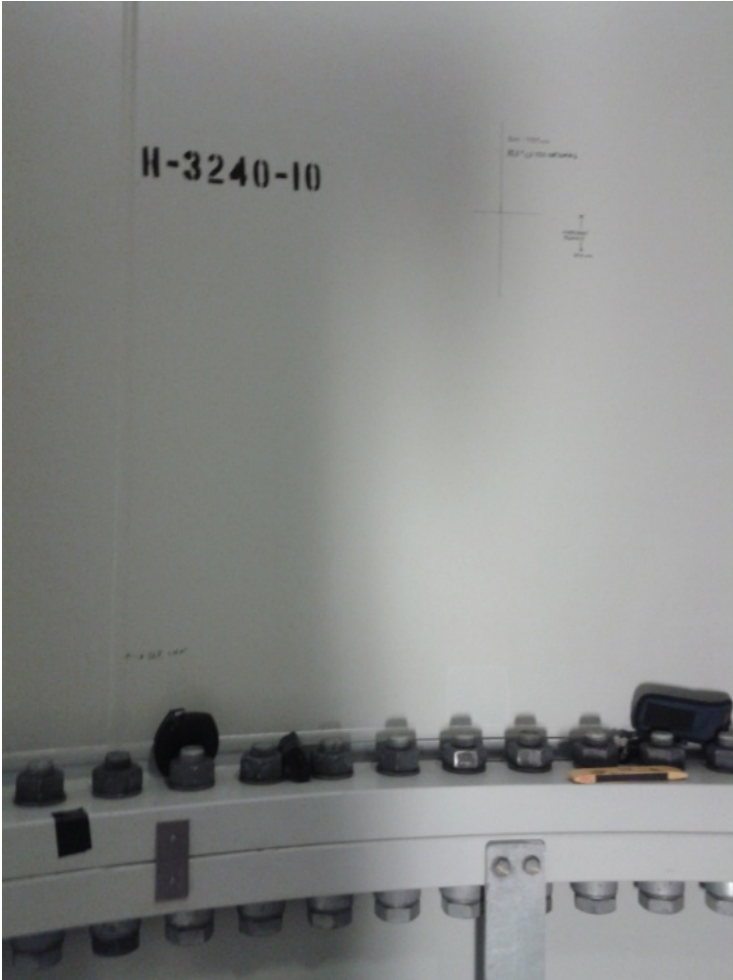
The strain gauge bridges (bending North / South - and East / West and torsion) are placed 1540 mm below the underside of the top flange, approximately 1640 mm from tower top.



Sensor names: **Torq\_TT, NS\_TT, EW\_TT**

**Tower middle:**

The strain gauge bridges (bending North / South and East / West) are placed 1000 mm above the top of the tower middle flange, approximately 35880 mm from the tower top.



Sensor names: **NS\_TM, EW\_TM**

**Tower Bottom:**

The strain gauge bridges (bending North / South and East / West) are placed 700 mm above the top edge of the tower base flange, approximately 58705 mm from the tower top.

Sensor names: **NS\_TB, EW\_TB**

### **Accelerations Tower middle**

An accelerometer measuring accelerations in three directions is placed on the tower wall 1200 mm above the top of the tower middle flange, approximately 35680 mm from the tower top.

Sensor names: **AccZ\_TM, AccX\_TM, AccY\_TM**

### **Accelerations Tower Bottom**

An accelerometer measuring accelerations in three directions is placed on the tower wall placed 900 mm above the top edge of the tower base flange, approximately 58505 mm from the tower top.



Sensor names: **AccZ\_TB, AccX\_TB, AccY\_TB.**

### **Power:**

A calibrated power transducer Deif MTR-2-415 has been installed together with current transducers by Siemens, the data has been sampled by DTU's measurement system. Due to a technical error the sensor was only working in the second half of the measurement period.

Sensor names: **Power, Reactive\_power, Voltage, Current.**

### **Pressure and Temperature on the footbridge:**

A pressure and a temperature sensor have been installed on the footbridge just outside of the entrance to the turbine.

Sensor names: **Press\_Bot, Tabs\_Bot.**



### **Transition piece**

The Transition piece is equipped with: Strain gauge bridges measuring bending in North / South and East / West direction at one height. One accelerometer measures accelerations in three directions. One inclinometer measures angle in two directions.

### **Strain gauge bridges**

The strain gauge bridges (bending North / South and East / West) are placed 2100 mm below the lower edge of the tower base flange, approximately 61795 mm from the tower top.

10 cm above highest strain gauge from the monopole/ Transition piece measurement system installed by DONG.



Sensor names: **NS\_Found, EW\_Found**

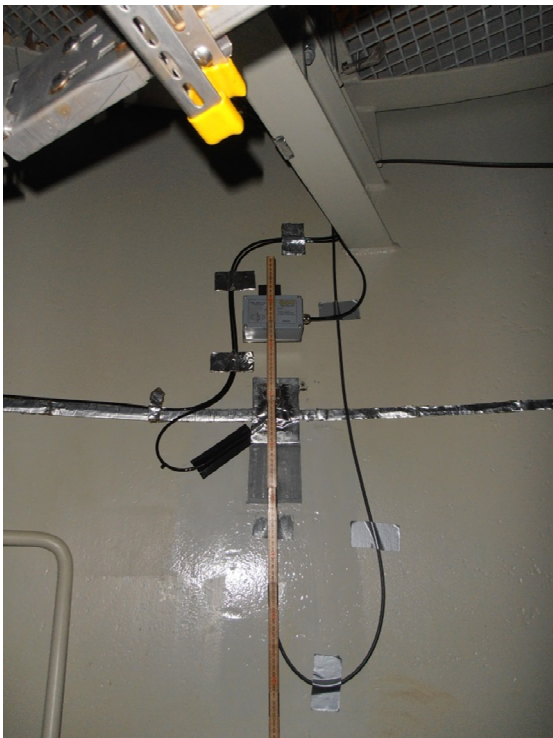
### **Accelerometer and Inclinometer**

An accelerometer measuring accelerations in three directions is placed on the tower wall 1850 mm below the lower edge of the tower base flange, approximately 61545 mm from the tower top.

### **Inclinometer**

An inclinometer measuring angle in two directions is placed on the tower wall 300 mm above the deck in the transition piece, approximately 63145 mm from the tower top.

Accelerometer



Sensor names: **AccZ\_F, AccX\_F, AccY\_F**

Inclinometer



Sensor names: **inc\_X\_NS, inc\_Y\_EW**

## Calibrations

Below is a table containing the set of calibration values for all sensors developed in the beginning of the measurement period. It should be treated as indicative, and where necessary recalculated for the measurement period that will be analysed especially considering that the load signals from the Strain gauge bridges can drift significantly in the offset value during time.

The calibration is linear as (Gain \* sensor value + offset), whose derivations are described in [[1]].

**Table 4.1: Calibration Results for all Installed Turbine Sensors**

Sensor	Gain	Offset
Flap blade A	3844	-340
Edge blade A	3928	-300
Flap blade B	4067	-400
Edge blade B	-3991	350
Flap blade C	3714	-200
Edge blade C	-3666	0
Shaft torque	1	-200000
Shaft 0-180	-4087	9.09
Shaft 90-270	-4203	141
Acc Z center	0.5	-1.6
Acc X center	0.5	-1.44
Acc Y center	0.5	1.46
Acc Z rear	0.5	-1.53
Acc X rear	0.5	-1.48
Acc Y rear	0.5	-1.44
Rotor position	1	180
Torq TT	10757	-860
NS TT	10000	975
EW TT	9914	-2645
NS TM	-30190	7045
EW TM	31525	-2488
NS TB	-47000	17202
EW TB	46577	-12822
NS foun	-71492	22070
EW foun	72500	-8530
Acc Z TM	-0.5	1.5225
Acc X TM	0.5	-1.4779
Acc Y TM	0.5	-1.425
Acc Z TB	-0.5	1.4815
Acc X TB	0.5	-1.42024
Acc Y TB	0.5	-1.47
Acc Z foun	-0.5	1.4767
Acc X foun	0.5	-1.4554

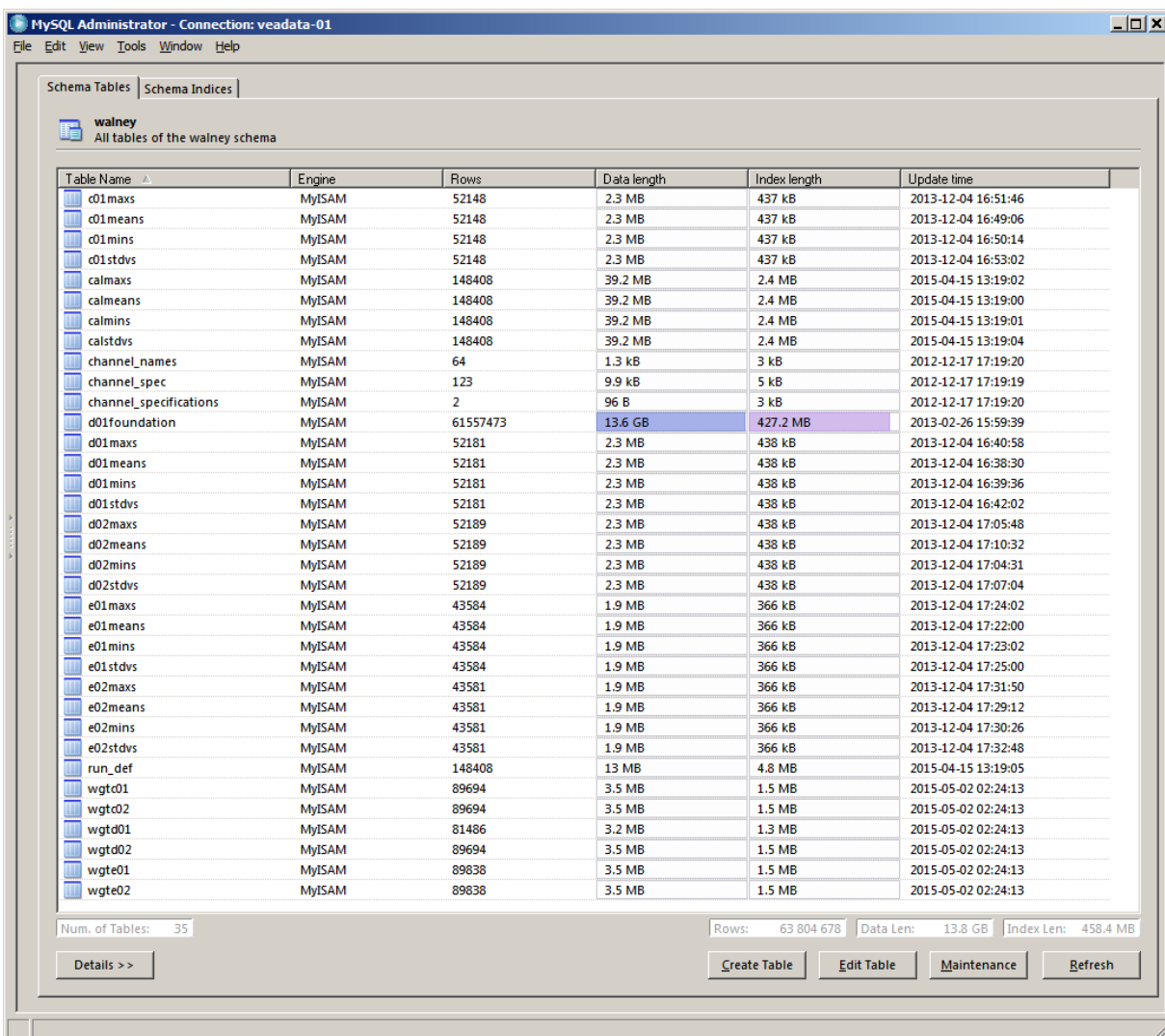
Acc Y foun	0.5	-1.441
Inc X NS	1.5	-4.79
Inc Y EW	1.5	-4.53
Power	450	-1800
Reactive_power	360	-3600
Voltage	2.5	0
Current	300	0

## 5.0 Description of Database of Measurements and Access

The databases containing the measurements for the Walney project are located on DTU's server:

**veadata-01.risoe.dk**

The databases are hosted using a MySQL server version 4.1.22. The data from the project are hosted in 2 separate databases: Walney and Walney\_public. The data in the Walney database contains the uncensored data from the campaign, and access to this database is restricted to the partners of the project. Below is a picture that depicts all the tables that contain data within the Walney database.



MySQL Administrator - Connection: veadata-01

Schema Tables | Schema Indices

walney  
All tables of the walney schema

Table Name	Engine	Rows	Data length	Index length	Update time
c01maxs	MyISAM	52148	2.3 MB	437 kB	2013-12-04 16:51:46
c01means	MyISAM	52148	2.3 MB	437 kB	2013-12-04 16:49:06
c01mins	MyISAM	52148	2.3 MB	437 kB	2013-12-04 16:50:14
c01stdvs	MyISAM	52148	2.3 MB	437 kB	2013-12-04 16:53:02
calmaxs	MyISAM	148408	39.2 MB	2.4 MB	2015-04-15 13:19:02
calmeans	MyISAM	148408	39.2 MB	2.4 MB	2015-04-15 13:19:00
calmins	MyISAM	148408	39.2 MB	2.4 MB	2015-04-15 13:19:01
calstdvs	MyISAM	148408	39.2 MB	2.4 MB	2015-04-15 13:19:04
channel_names	MyISAM	64	1.3 kB	3 kB	2012-12-17 17:19:20
channel_spec	MyISAM	123	9.9 kB	5 kB	2012-12-17 17:19:19
channel_specifications	MyISAM	2	96 B	3 kB	2012-12-17 17:19:20
d01foundation	MyISAM	61557473	13.6 GB	427.2 MB	2013-02-26 15:59:39
d01maxs	MyISAM	52181	2.3 MB	438 kB	2013-12-04 16:40:58
d01means	MyISAM	52181	2.3 MB	438 kB	2013-12-04 16:38:30
d01mins	MyISAM	52181	2.3 MB	438 kB	2013-12-04 16:39:36
d01stdvs	MyISAM	52181	2.3 MB	438 kB	2013-12-04 16:42:02
d02maxs	MyISAM	52189	2.3 MB	438 kB	2013-12-04 17:05:48
d02means	MyISAM	52189	2.3 MB	438 kB	2013-12-04 17:10:32
d02mins	MyISAM	52189	2.3 MB	438 kB	2013-12-04 17:04:31
d02stdvs	MyISAM	52189	2.3 MB	438 kB	2013-12-04 17:07:04
e01maxs	MyISAM	43584	1.9 MB	366 kB	2013-12-04 17:24:02
e01means	MyISAM	43584	1.9 MB	366 kB	2013-12-04 17:22:00
e01mins	MyISAM	43584	1.9 MB	366 kB	2013-12-04 17:23:02
e01stdvs	MyISAM	43584	1.9 MB	366 kB	2013-12-04 17:25:00
e02maxs	MyISAM	43581	1.9 MB	366 kB	2013-12-04 17:31:50
e02means	MyISAM	43581	1.9 MB	366 kB	2013-12-04 17:29:12
e02mins	MyISAM	43581	1.9 MB	366 kB	2013-12-04 17:30:26
e02stdvs	MyISAM	43581	1.9 MB	366 kB	2013-12-04 17:32:48
run_def	MyISAM	148408	13 MB	4.8 MB	2015-04-15 13:19:05
wgtc01	MyISAM	89694	3.5 MB	1.5 MB	2015-05-02 02:24:13
wgtc02	MyISAM	89694	3.5 MB	1.5 MB	2015-05-02 02:24:13
wgtd01	MyISAM	81486	3.2 MB	1.3 MB	2015-05-02 02:24:13
wgtd02	MyISAM	89694	3.5 MB	1.5 MB	2015-05-02 02:24:13
wgte01	MyISAM	89838	3.5 MB	1.5 MB	2015-05-02 02:24:13
wgte02	MyISAM	89838	3.5 MB	1.5 MB	2015-05-02 02:24:13

Num. of Tables: 35 | Rows: 63 804 678 | Data Len: 13.8 GB | Index Len: 458.4 MB

Details >> | Create Table | Edit Table | Maintenance | Refresh

Figure 5.1 Snapshot of tables in database

The walney\_public database contains the unrestricted version of the data:

In order to get access to the database, it is necessary to install relevant client software on the user's computer. There are several types of client software available: MySQL administrator, MySQL query browser, HeidiSQL, SQLyog, and probably others. NOTE! The **MySQL workbench** software does not work with this version of the SQL database. If a graphical user interface is not needed by the user, then other software (e.g. Matlab, Mathematica) can be used so long as the MySQL ODBC driver is installed.

The information needed to connect to the database are:

1. A user name
2. A password
3. The connection endpoint (which is: veadata-01.risoe.dk on MySQL default port 3306).

The user name and password can be obtained from the project management group (anat@dtu.dk)

## Description of data in the walney database

### Database and tables

The data is stored in tables as in Fig. 5.1 and represents the 10 minute statistics on loads, waves and wind measured on the instrumented turbine and 10 minute averaged SCADA information from 4 surrounding wind turbines situated in the Walney offshore wind farm. The turbines have ID numbers: C01, D01, D02, E01 and E02 – their positions inside the farm can be seen in Fig. 5.2.

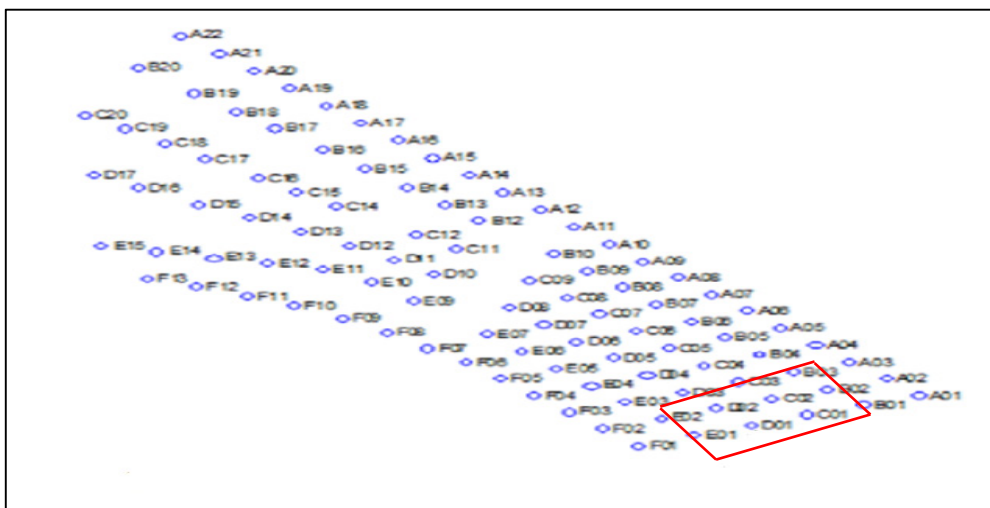


Figure 3.2 Layout of Walney offshore wind farm showing the wind turbines within the red rectangle that are accessed in the database.

The data from each turbine is placed in four different tables with mean values, std. deviation values, maximum values and minimum values. All tables contain the same columns and they are described in the table below. The statistical averaging period is 10min.

**Table 5.2 Names of the tables for each wind turbine**

WT id number	Table names			
	Mean values	Std values	Maximum values	Minimum values
C01	c01means	c01stdvs	c01maxs	c01mins
D01	d01means	d01stdvs	d01maxs	d01mins
D02	d02means	d02stdvs	d02maxs	d02mins
E01	e0means	e01stdvs	e01maxs	e01mins
E02	e02means	e02stdvs	e02maxs	e02mins

**Table 5.2 Columns and units in the 10min statistics tables**

Column name	Units	Comments
Name	yyyymmddhhmm	Timestamp
ActivePower	kW	Active power
BladeAngleA	deg	Pitch angle of blade A
BladeAngleB	deg	Pitch angle of blade B
BladeAngleC	deg	Pitch angle of blade C
RotorRPM	Rpm	Rotational speed of the rotor
YawDirection	Deg	Wind turbine yaw direction

### Time stamp and Periods of Available Data

The time stamp on the data in the tables corresponds to: UTC + 1h and the below tables provide the available periods of measurement.

**Table 5.3 Minimum and maximum time stamp in the tables for the five wind turbines**

Turbine ID	Start	End
C01	01-01-2012 00:04	31-12-2012 23:53
D01	01-01-2012 00:03	31-12-2012 23:56
D02	01-01-2012 00:00	31-12-2012 23:50
E01	01-03-2012 00:04	31-12-2012 23:52

E02	01-03-2012 00:00	31-12-2012	56
-----	------------------	------------	----

**Table 5.4 Periods with missing data for each turbine:**

Turbine	Start	End	Number of days
C01	02-11-2012 09:40	03-11-2012 15:10	1.23
D01	02-11-2012 09:40	03-11-2012 15:10	1.23
	27-11-2012 16:50	28-11-2012 08:30	0.65
D02	02-11-2012 10:10	03-11-2012 15:20	1.21
	27-11-2012 16:50	28-11-2012 08:40	0.66
E01	02-11-2012 10:10	03-11-2012 15:20	1.21
	27-11-2012 16:50	28-11-2012 08:30	0.65
E02	02-11-2012 10:10	03-11-2012 15:20	1.21
	27-11-2012 16:50	28-11-2012 08:30	0.65

It should be noted that the indicated period of missing data means that the measurement system was not working at all. However it does not guarantee that all sensors were working properly during the rest of the time. This should be additionally checked before analyzing the data.

### Calibrations

The data in all tables is given in its appropriate units and there is no need to further calibrate the data.

### Description of Tables wgtc01, wgtc02, wgtD01, wgtD02, wgte01, wgte02

All these six tables contain SCADA information averaged over 10 minutes with the same columns and they are described in the table below. The averaging period is 10min.

**Table 5.5 Columns and units in the Scada data tables**

Column name	Units	Comments
Name	yyyymmddhhmm	Timestamp
ActivePower	kW	Active power
BladeAngleA	deg	Pitch angle of blade A
BladeAngleB	deg	Pitch angle of blade B
BladeAngleC	deg	Pitch angle of blade C
RotorRPM	Rpm	Rotational speed of the rotor



YawDirection	Deg	Wind turbine yaw direction
--------------	-----	----------------------------

### Time stamp

The time stamp on the data in the tables corresponds to **CEST** (Central European Summer Time). During summer there is an offset of 1 hour between the SCADA system and DTU measurement system.

### Available data

**Table 5.6 Minimum and maximum time stamp in the tables for all six wind turbines**

Turbine ID	Start	End
C01	07-06-2012 00:00	16-10-2014 23:50
C02	07-06-2012 00:00	16-10-2014 23:50
D01	25-11-2012 00:00	16-10-2014 23:50
D02	07-06-2012 00:00	16-10-2014 23:50
E01	07-06-2012 00:00	16-10-2014 23:50
E02	07-06-2012 00:00	16-10-2014 50

**Table 5.7 Periods with missing data for each turbine:**

Table	Start	End	Number of days
WGTC01	24-06-2012 00:00	14-10-2012 00:00	112
	27-10-2012 00:00	29-10-2012 00:00	2
	22-11-2012 00:00	24-11-2012 00:00	2
	05-01-2013 00:00	10-01-2013 00:00	5
	10-01-2013 00:00	29-01-2013 00:00	19
	29-01-2013 00:00	17-02-2013 00:00	19
	17-02-2013 00:00	04-04-2013 00:00	46
	26-04-2013 00:00	28-04-2013 00:00	2
	29-04-2013 00:00	01-05-2013 00:00	2
	19-05-2013 00:00	21-05-2013 00:00	2
	20-06-2013 00:00	24-06-2013 00:00	4
16-02-2014 00:00	28-09-2014 00:00	224	
WGTC02	24-06-2012 00:00	14-10-2012 00:00	112
	27-10-2012 00:00	29-10-2012 00:00	2
	22-11-2012 00:00	24-11-2012 00:00	2
	05-01-2013 00:00	10-01-2013 00:00	5
	10-01-2013 00:00	29-01-2013 00:00	19

	29-01-2013 00:00	17-02-2013 00:00	19
	17-02-2013 00:00	04-04-2013 00:00	46
	26-04-2013 00:00	28-04-2013 00:00	2
	29-04-2013 00:00	01-05-2013 00:00	2
	19-05-2013 00:00	21-05-2013 00:00	2
	20-06-2013 00:00	24-06-2013 00:00	4
	16-02-2014 00:00	28-09-2014 00:00	224
WGTD01	05-01-2013 00:00	10-01-2013 00:00	5
	10-01-2013 00:00	29-01-2013 00:00	19
	29-01-2013 00:00	17-02-2013 00:00	19
	17-02-2013 00:00	04-04-2013 00:00	46
	26-04-2013 00:00	28-04-2013 00:00	2
	29-04-2013 00:00	01-05-2013 00:00	2
	19-05-2013 00:00	21-05-2013 00:00	2
	20-06-2013 00:00	24-06-2013 00:00	4
	16-02-2014 00:00	28-09-2014 00:00	224
WGTC02	24-06-2012 00:00	14-10-2012 00:00	112
	27-10-2012 00:00	29-10-2012 00:00	2
	22-11-2012 00:00	24-11-2012 00:00	2
	05-01-2013 00:00	10-01-2013 00:00	5
	10-01-2013 00:00	29-01-2013 00:00	19
	29-01-2013 00:00	17-02-2013 00:00	19
	17-02-2013 00:00	04-04-2013 00:00	46
	26-04-2013 00:00	28-04-2013 00:00	2
	29-04-2013 00:00	01-05-2013 00:00	2
	19-05-2013 00:00	21-05-2013 00:00	2
	20-06-2013 00:00	24-06-2013 00:00	4
	16-02-2014 00:00	28-09-2014 00:00	224
WGTE01	24-06-2012 00:00	14-10-2012 00:00	112
	27-10-2012 00:00	29-10-2012 00:00	2
	22-11-2012 00:00	24-11-2012 00:00	2
	05-01-2013 00:00	10-01-2013 00:00	5
	10-01-2013 00:00	29-01-2013 00:00	19
	29-01-2013 00:00	17-02-2013 00:00	19
	17-02-2013 00:00	04-04-2013 00:00	46
	26-04-2013 00:00	28-04-2013 00:00	2
	29-04-2013 00:00	01-05-2013 00:00	2
	19-05-2013 00:00	21-05-2013 00:00	2
	20-06-2013 00:00	24-06-2013 00:00	4
	16-02-2014 00:00	28-09-2014 00:00	224

WGTE02	24-06-2012 00:00	14-10-2012 00:00	112
	27-10-2012 00:00	29-10-2012 00:00	2
	22-11-2012 00:00	24-11-2012 00:00	2
	05-01-2013 00:00	10-01-2013 00:00	5
	10-01-2013 00:00	29-01-2013 00:00	19
	29-01-2013 00:00	17-02-2013 00:00	19
	17-02-2013 00:00	04-04-2013 00:00	46
	26-04-2013 00:00	28-04-2013 00:00	2
	29-04-2013 00:00	01-05-2013 00:00	2
	19-05-2013 00:00	21-05-2013 00:00	2
	20-06-2013 00:00	24-06-2013 00:00	4
	16-02-2014 00:00	28-09-2014 00:00	224

It should be noted that the indicated period of missing data means that the measurement system was not working at all. However it does not guarantee that all sensors were working during the rest of the time. This should be additionally checked before analyzing the data.

### Calibrations

The data in all six tables is given in its appropriate units and there is no need to further process the data.

### Load measurements from turbine D01

- 1) The data from the loads measurements from the turbine itself is placed in four different tables – with mean values, std values, maximum values and minimum values. All tables contain the same columns and they are described in the table below. The statistical period is 10min. The sampling frequency is 35Hz.

**Table 5.8 Columns and units in the 10min Load data statistics tables**

Column name	Units	Comments
Name	yyyymmddhhmm	Timestamp
Spin_stat	[-]	Status signal, values between 0 and 4
Flap_bIA	[V]	Flapwise bending moment of

		blade A;
Edge_bIA	[V]	Edgewise bending moment of blade A;
Flap_bIB	[V]	Flapwise bending moment of blade B;
Edge_bIB	[V]	Edgewise bending moment of blade B;
Flap_bIC	[V]	Flapwise bending moment of blade C;
Edge_bIC	[V]	Edgewise bending moment of blade C;
Shaft_torq	[V]	Shaft torque (“not working” – comment from Kristina’s thesis)
Shaft_0m180	[V]	Bending moment in the main shaft, 0-180 degrees direction
Shaft_90m270	[V]	Bending moment in the main shaft, 90-270 degrees direction
Nac_stat	[-]	Nacelle status signal; between 0 and 4
AccZ_center	[V]	Acceleration of the center of the nacelle along the Z axis
AccX_center	[V]	Acceleration of the center of the nacelle along the X axis
AccY_center	[V]	Acceleration of the center of the nacelle along the Y axis
AccZ_rear	[V]	Acceleration of the rear of the nacelle along the Z axis
AccX_rear	[V]	Acceleration of the rear of the nacelle along the X axis
AccY_rear	[V]	Acceleration of the rear of the nacelle along the Y axis
LS_Shaft	[RPM]	Low speed shaft rotational speed
HS_shaft	[RPM]	High speed shaft rotational speed
Rotor_pos	[Deg]	0 azimuth = blade 1 upright position
Wsp_thies	[m/s]	Thies cup anemometer
SWP_wsp	[m/s]	Siemens cup anemometer; needs transfer function
SWP_gen	[-]	Needs transfer function

Tower1_stat	[-]	
Torq_TT	[V]	Tower top, torsion
NS_TT	[V]	Tower top bending moment, North-South fixed system
EW_TT	[V]	Tower top bending moment, East-West fixed system
NS_TM	[V]	Tower middle bending moment, North-South fixed system
EW_TM	[V]	Tower middle bending moment, East-West fixed system
NS_TB	[V]	Tower bottom bending moment, North-South fixed system
EW_TB	[V]	Tower bottom bending moment, East-West fixed system
NS_Found	[V]	Transition piece bending moment, North-South fixed system
EW_Found	[V]	Transition piece bending moment, East-West fixed system
Power	[V]	Analog output 1 from the power transducer, total real power (Sensor in operation after 20121217)
Reactive_power	[V]	Analog output 2 from the power transducer, total reactive power
Voltage	[V]	Analog output 3 from the power transducer; voltage measured between L1 and N
Current	[V]	Analog output 4 from the power transducer, current measured on L1
Tabs_Bot	[°C]	Absolute temperature measured outside, at the transition piece
Press_bot	[hPa]	Pressure measured outside, at the transition piece
Tower2_stat	[-]	Data logger status signal
AccZ_TM	[V]	Accelariotn of of the middle of the tower along the Z axis
AccX_TM	[V]	Accelariotn of of the middle of the tower along the X axis
AccY_TM	[V]	Accelariotn of of the middle of

		the tower along the Y axis
AccZ_TB	[V]	Acceleration of the bottom of the tower along the Z axis
AccX_TB	[V]	Acceleration of the bottom of the tower along the X axis
AccY_TB	[V]	Acceleration of the bottom of the tower along the Y axis
AccZ_F	[V]	Acceleration of the foundation of the turbine along the Z axis
AccX_F	[V]	Acceleration of the foundation of the turbine along the X axis
AccY_F	[V]	Acceleration of the foundation of the turbine along the Y axis
Inc_X_NS	?	Inclinometer, transition piece, North South
Inc_Y_EW	?	Inclinometer, transition piece, East West
Azimuth	[deg]	Rotor position
PosA	[deg]	Pitch angle blade A
PosB	[deg]	Pitch angle blade B
PosC	[deg]	Pitch angle blade C
RefA	[deg]	Pitch angle blade A, requested by the controller
RefB	[deg]	Pitch angle blade B, requested by the controller
RefC	[deg]	Pitch angle blade C, requested by the controller
ModuleStatus	[-]	Status signal, values between 0 and 4
YAW	[deg]	Yaw direction
RH_top	[%]	Relative humidity, on the nacelle
Vaisala_temp_top	[°C]	Temperature, on top of the nacelle (same sensor as for RH_top)
Press_top	[hPa]	Pressure sensor, on top of the nacelle
Tabs_top	[°C]	Temperature sensor, on top of the nacelle

- 2) Additional information regarding the tables calmeans, calstdvs, calmins and calmaxs is placed in the following tables: channel\_names, channel\_spec, channel\_specifications. The following tables provide description of the tables.

**Table 5.9 Columns and units in table “channel\_names”**

Column name	Units	Comments
Chan_name	[-]	Names of the columns from “calmeans” table
In_use	[True/False]	It’s either T or F. T means that the channel is currently in use. F means that the channel is no longer in use.

**Table 5.10 Columns and units in table “channel\_spec”**

Column name	Units	Comments
List_version	[-]	
List_index	[-]	
Chan_index	[-]	Number of the channel in daqwin setup file
Chan_name	[-]	Channel name in daqwin setup file
Description	[-]	Description of the channel
Units	[-]	Units in which the variable is measured
Height_m	[-]	Height at which the instrument is placed
Changed	[True/False]	Shows whether the instrument was changed or not during the measurements
New	[True/False]	Shows if the instrument is new or if it has already been used before.
Frequency	[-]	Sampling frequency
Fast_saved	[True/False]	Shows if the raw data is saved in the database or not

Instr_make	[-]	Make of the instrument
Instr_type	[-]	Type of the instrument
Instr_sn	[-]	Serial number of the instrument
Instr_cal_A	[-]	
Instr_cal_B	[-]	
Instr_cal_b	[-]	
Instr_cal_c	[-]	
Cond_make	[-]	
Cond_type	[-]	
Cond_sn	[-]	
Line_gain	[-]	Gain applied in daqwin
Line_offset	[-]	Offset applied in daqwin
Logger_id	[-]	ID number of the logger
Structure_id	[-]	
Component	[-]	
Location	[-]	
Boom_length_m	[-]	Length of the boom
Boom_dir	[deg]	Orientation of the boom
Height_above_boom	[-]	Shows how much above the boom the instrument is placed
Top_mount	[True/False]	Shows whether the instrument is top mounted or not
Missing_data	[-]	
Variable_id	[-]	
Status_comment	[-]	
Setup_comment	[-]	

**Table 5.11 Columns and units in table “channel\_specifications”**

Column name	Units	Comments
List_version	[-]	Version name of the settings of the measurement system.
Valid_from	Yyyy-mm-dd hh:mm:ss	Shows when the settings of the measurement system were changed
List_version	[-]	Version number of the settings of the measurement system.
Time_zone	[-]	Shows which time zone the



		timestamp corresponds to.
Comment	[-]	Additional comments

### Time stamp

The time stamp on the data in the tables corresponds to:

UTC + 1h

### Available data

**Table 5.12 Minimum and maximum time stamp in the tables**

Table name	Start	End
D01 Turbine Loads calmeans	12-06-2012 15:40	28-02-2015 15:00
D01foundation	31-05-2012 23:52	10-01-2013 01

**Table 5.13 Periods with missing data:**

Tables	Start	End	Number of days
D01 Turbine Loads calmeans	02-11-2012 16:30	03-11-2012 15:00	0.94
D01foundation	06-07-2012 22:29	10-01-2013 10:50	187.5

It should be noted that the indicated period of missing data means that the measurement system was not working at all. However it does not guarantee that all sensors were working during the rest of the time. This should be additionally checked before analyzing the data.

### Calibrations

All of the channels corresponding to load measurements are given in units [V]. The calibration gains and offsets are presented in the previous chapter under table 4.1.

### Foundation load measurements on turbine D01

The data from the loads measurements on the wind turbine foundation are placed in a table called D01foundation. A description of this table can be found in Table 5.55. The statistical period is 10min. The sampling frequency is 20Hz.

**Table 5.55 Columns and units in table D01 foundation loads measurements**

Column name	Units	Comments
Name	yyyymmddhhmm	Time stamp, UTC +1
Scan_id	[-]	Sample number within each 10min period
channel1	[ $\mu\text{m}/\text{m}$ ]	SG 19.5 60 CH=4
channel2	[ $\mu\text{m}/\text{m}$ ]	SG 19.5 150 CH=5
channel3	[ $\mu\text{m}/\text{m}$ ]	SG 19.5 240 CH=6
channel4	[ $\mu\text{m}/\text{m}$ ]	SG 19.5 330 CH=7
channel5	[ $\mu\text{m}/\text{m}$ ]	SG 6.5 60 CH=8
channel6	[ $\mu\text{m}/\text{m}$ ]	SG 6.5 150 CH=9
channel7	[ $\mu\text{m}/\text{m}$ ]	SG 6.5 240 CH=10
channel8	[ $\mu\text{m}/\text{m}$ ]	SG 6.5 330 CH=11
channel9	[ $\mu\text{m}/\text{m}$ ]	SG -19.4 60 CH=12
channel10	[ $\mu\text{m}/\text{m}$ ]	SG -19.4 150 CH=13
channel11	[ $\mu\text{m}/\text{m}$ ]	SG -19.4 240 CH=14
channel12	[ $\mu\text{m}/\text{m}$ ]	SG -19.4 330 CH=15
channel13	[ $\mu\text{m}/\text{m}$ ]	SG -23.4 60 CH=16
channel14	[ $\mu\text{m}/\text{m}$ ]	SG -23.4 150 CH=17
channel15	[ $\mu\text{m}/\text{m}$ ]	SG -23.4 240 CH=18
channel16	[ $\mu\text{m}/\text{m}$ ]	SG -23.4 330 CH=19
channel17	[ $\mu\text{m}/\text{m}$ ]	SG -25.5 60 CH=20
channel18	[ $\mu\text{m}/\text{m}$ ]	SG -25.4 150 CH=21
channel19	[ $\mu\text{m}/\text{m}$ ]	SG -25.4 240 CH=22
channel20	[ $\mu\text{m}/\text{m}$ ]	SG -25.4 330 CH=23
channel21	[ $\mu\text{m}/\text{m}$ ]	SG -27.4 60 CH=24
channel22	[ $\mu\text{m}/\text{m}$ ]	SG -27.4 150 CH=25
channel23	[ $\mu\text{m}/\text{m}$ ]	SG -27.4 240 CH=26
channel24	[ $\mu\text{m}/\text{m}$ ]	SG -27.4 330 CH=27
channel25	[ $\mu\text{m}/\text{m}$ ]	SG -29.4 60 CH=28
channel26	[ $\mu\text{m}/\text{m}$ ]	SG -29.4 150 CH=29
channel27	[ $\mu\text{m}/\text{m}$ ]	SG -29.4 240 CH=30
channel28	[ $\mu\text{m}/\text{m}$ ]	SG -29.4 330 CH=31
channel29	[ $\mu\text{m}/\text{m}$ ]	SG -31.4 60 CH=32
channel30	[ $\mu\text{m}/\text{m}$ ]	SG -31.4 150 CH=33
channel31	[ $\mu\text{m}/\text{m}$ ]	SG -31.4 240 CH=34
channel32	[ $\mu\text{m}/\text{m}$ ]	SG -31.4 330 CH=35

channel33	[ $\mu\text{m}/\text{m}$ ]	SG -33.4 60 CH=36
channel34	[ $\mu\text{m}/\text{m}$ ]	SG -33.4 150 CH=37
channel35	[ $\mu\text{m}/\text{m}$ ]	SG -33.4 240 CH=38
channel36	[ $\mu\text{m}/\text{m}$ ]	SG -33.4 330 CH=39
channel37	[ $\mu\text{m}/\text{m}$ ]	SG -35.4 60 CH=40
channel38	[ $\mu\text{m}/\text{m}$ ]	SG -35.4 150 CH=41
channel39	[ $\mu\text{m}/\text{m}$ ]	SG-35.4 240 CH=42
channel40	[ $\mu\text{m}/\text{m}$ ]	SG -35.4 330 CH=43
channel41	[ $\mu\text{m}/\text{m}$ ]	SG -39.4 60 CH=44
channel42	[ $\mu\text{m}/\text{m}$ ]	SG -39.4 150 CH=45
channel43	[ $\mu\text{m}/\text{m}$ ]	SG -39.4 240 CH=46
channel44	[ $\mu\text{m}/\text{m}$ ]	SG -39.4 330 CH=47
channel45	[g]	ACC 19.5 60 CH=52
channel46	[g]	ACC 19.5 150 X CH=53
channel47	[g]	ACC 19.5 150 Y CH=54
channel48	[g]	ACC 6.5 60 CH=55
channel49	[g]	ACC 6.5 150 X CH=56
channel50	[g]	ACC 6.5 150 Y CH=57
channel51	[ $^{\circ}$ ]	INC 19.5 NS CH=58
channel52	[ $^{\circ}$ ]	INC 19.5 EW CH=59
channel53	[mm]	LASER 6.5 MEAS CH=60
channel54	[mm]	LASER 6.5 REF CH=61

### Time stamp

The time stamp in the database corresponds to UTC+1h + 50minutes

### Available data

**Table 16 Minimum and maximum time stamp in the tables**

Table name	Start	End
D01foundation	31-05-2012 23:52	10-01-2013 01

**Table 17 Periods with missing data:**

Tables	Start	End	Number of days
D01foundation	06-07-2012 22:29	10-01-2013 10:50	187.5

It should be noted that the indicated period of missing data means that the measurement system was not working at all. However it does not guarantee that all sensors were working properly during the rest of the time. This should be additionally checked before analyzing the data.

## Calibrations

The foundation data are provided as strains. The strain gauges are 4 per height placed one across each other at 90° connecting half bridges to full bridges. There are a total of 44 strain gauges at 11 heights along the transition piece, the monopile and the pilesand. The calibration is separated in two periods, March-July 2012 and December 2012-February 2013. For the first period the offsets are based on a yaw test performed in September 2011 and internal communication. The expression for the calibration of the strains is given by 5. 1, where  $strain_{raw}$  is the measurement from the wind farm,  $e_{yaw}$  is the strain offset from the yaw test,  $e_{yawzero}$ ,  $e_{zero}$ ,  $e_{yawtare}$  and  $e_{tare}$  are parameters of the instrumentation. The values for the calibration of each strain gauge are given in Table 18. The first number in the name of each strain gauge (ex. SG 19.5 60) shows the height and the second the orientation. The direction has been wrongly assigned to the data due to a mirroring of the monopile during strain gauge installation (internal communication). Therefore, a shift of the columns is required.

$$strain = strain_{raw} - e_{yaw} - (e_{yawzero} - e_{zero}) - (e_{yawtare} - e_{tare}) \quad - \quad 5.1$$

**Table 5.18 Offsets for the foundation strain gauges March-July 2012**

Name	Offset	$e_{yawzero}$	$e_{yawtare}$	$e_{zero}$	$e_{tare}$
SG 19.5 60	-419.46	440.14	440.77	731.78	440.77
SG 19.5 150	-461.88	459.39	463.34	463.75	464.34
SG 19.5 240	-266.22	287.03	275.01	308.92	0
SG 19.5 330	-1.28	-43.58973	0	-50.7299	0
SG 6.5 60	17.59	-14.2549	0	2.77355	0
SG 6.5 150	-461.34	469.26	470.52	481.26	470.52
SG 6.5 240	-562.35	574.32	570.27	586.77	570.27
SG 6.5 330	115.12	-103.453	-106.3213	-97.6771	0
SG -19.4 60	-156.16	-143.8753	-145.221	-150.698	-145.221
SG -19.4 150	180.39	-168.444	-170.4112	-149.499	-170.411
SG -19.4 240	-96.71	115.65	108.34	133.02	108.34
SG -19.4 330	NaN	281.2	275.55	281.2	275.55
SG -23.4 60	178.19	-165.6384	-165.4163	-597.8549	-165.4163

SG -23.4 150	-129.55	140.77	139.76	161.45	139.76
SG -23.4 240	-221.23	174.42	167.4	174.42	167.4
SG -23.4 330	NaN	293.87	288.74	293.87	288.74
SG -25.5 60	40.82	-42.8599	-46.7187	-52.47524	-46.7187
SG -25.4 150	NaN	37.47143	-137.821	37.47142	-137.821
SG -25.4 240	NaN	-212.7951	-155.636	-212.795	-155.636
SG -25.4 330	NaN	0	0	0	0
SG -27.4 60	-175.15	173.01	170.85	160.45	170.85
SG -27.4 150	87.85	-89.00101	-90.91774	-76.11069	-90.91774
SG -27.4 240	273.81	-265.8161	-273.623	-260.4341	-273.623
SG -27.4 330	131.62	-124.797	-131.1944	-112.776	-131.1944
SG -29.4 60	65.54	-62.4397	-61.9637	-54.06194	-61.9367
SG -29.4 150	73.7	-67.36481	-66.66032	-67.3648	-66.66032
SG -29.4 240	171.56	-156.0802	-160.231	-132.4892	-160.231
SG -29.4 330	NaN	-289.807	-294.161	-289.807	-294.161
SG -31.4 60	NaN	-4166.779	0	-4166.779	0
SG -31.4 150	NaN	0	215.26	0	215.26
SG -31.4 240	524.86	-508.359	-511.1322	-475.5521	-511.1322
SG -31.4 330	250.47	-247.265	-250.051	-251.8532	-250.051
SG -33.4 60	NaN	-99.86671	-104.532	-99.8667	-104.532
SG -33.4 150	93.09	-87.07159	-90.04823	-68.0884	-90.04823
SG -33.4 240	20.72	-4.29678	-11.31	23.8195	-11.31
SG -33.4 330	512.04	-499.315	-507.8573	-496.541	-507.8573
SG -35.4 60	NaN	0	0	0	0
SG -35.4 150	67.83	-61.7606	-65.8162	-52.6847	-65.8162
SG -35.4 240	39.27	-21.09672	-29.6776	12.3826	-29.6776
SG -35.4 330	646.76	-635.58	-642.4409	-622.3194	-642.4409
SG -39.4 60	NaN	11293.2	0	11293.2	0
SG -39.4 150	-141.21	148.08	146	158.55	146
SG -39.4 240	NaN	0	0	0	0
SG -39.4 330	8.82	25.9076	0	25.9076	0

For the second period the strain offset is measured from a yaw test performed in January 2013. The calibration is given by  $-5.12$  and the offset values are in 19.

$$strain = strain_{raw} - e_{yaw} \quad -5.12$$

**Table 5.19 Offsets for the foundation strain gauges December 2012 – February 2013**

Name	Offset
SG 19.5 60	-706.1
SG 19.5 150	-461.6
SG 19.5 240	-5.541
SG 19.5 330	6.106
SG 6.5 60	2.139
SG 6.5 150	-469.8
SG 6.5 240	-577.4
SG 6.5 330	0.5331
SG -19.4 60	154.5
SG -19.4 150	166
SG -19.4 240	-108.1
SG -19.4 330	0
SG -23.4 60	0
SG -23.4 150	-401.5
SG -23.4 240	0
SG -23.4 330	0
SG -25.5 60	59.16
SG -25.4 150	0
SG -25.4 240	0
SG -25.4 330	0
SG -27.4 60	-158.9
SG -27.4 150	93.58
SG -27.4 240	260.5
SG -27.4 330	136.5
SG -29.4 60	96.74
SG -29.4 150	0
SG -29.4 240	149.8
SG -29.4 330	0
SG -31.4 60	0
SG -31.4 150	0
SG -31.4 240	504.8
SG -31.4 330	251.5
SG -33.4 60	0
SG -33.4 150	94.5
SG -33.4 240	3.84
SG -33.4 330	510.5
SG -35.4 60	0
SG -35.4 150	65.8

SG-35.4 240	33.7
SG -35.4 330	650.6
SG -39.4 60	0
SG -39.4 150	147.1
SG -39.4 240	0
SG -39.4 330	12.3

### Description of data in the walney\_public database

The walney\_public database also contains the wind data from the six turbines C01, C02, D01, D02, E01, E02, however any turbine specific data, except the yaw direction, is removed. The measurements on turbine D01 is also been provides as only contain meterological data and yaw direction. In addition to these data, there are data from a wind IRIS Lidar, and data from a wave measuring buoy.

### Wind LIDAR Iris data

The tables iris\_meanstdv3\_b0, iris\_meanstdv3\_b1 and wind\_iris\_10min contain 10 min. statistical data. The table Wind\_iris\_fast2 contains 1 Hz time series data.

**Table 5.20 Columns and units in the nacelle lidar tables: iris\_meanstdv3\_b0 and iris\_meanstdv3\_b1**

Column name	Units	Comments
Name	yyyymmddhhmm	Timestamp
D_T	Yyyy-mm-dd tt:mm:ss	Timestamp;
Distance	m	Horizontal distance between the lidar and point of measurements
HWS	m/s	Horizontal wind speed; see note below
Dir	°	Direction; it is in the range of [-180÷180] deg;
RWS	m/s	Radial wind speed, mean
RWSD	m/s	Average of the 1Hz measurement of RWSD
CNR	dB	Carrier to noise ratio
Tilt	°	Tilt angle of the lidar
Roll	°	Roll angle of the lidar
RWSStatus	-	

RWSRTStatus	-	All have values between 0 and 1
HWSStatus	-	
HWSRTStatus	-	
OverrunStatus	-	
HWS_stdv	m/s	Standard deviation of the horizontal wind speed; see note below
Dir_stdv	°	Standard deviation of the wind direction
RWS_stdv	m/s	Standard deviation of the 1Hz measurements of RWS

**Table 5.21 Columns and units in the nacelle lidar table windiris\_fast2 (1Hz.)**

Column name	Units	Comments
Timestamp	Yyyy-mm-dd hh:mm:ss	Timestamp
Distance	m	Horizontal distance between the lidar and the point of measurements
HWS	m/s	Horizontal wind speed
Dir	°	Direction; it is in the range of [-180÷180] deg;
RWS	m/s	Radial wind speed
RWSD	m/s	Standard deviation of the radial velocity within the probe volume of the lidar
CNR	dB	Carrier to noise ratio
Tilt	°	Tilt angle of the lidar
Roll	°	Roll angle of the lidar
RWSStatus	-	All have values between 0 and 1
RWSRTStatus	-	
HWSStatus	-	
HWSRTStatus	-	
OverrunStatus	-	



**Additional clarifications regarding the lidar data**

- RWSStatus: if it's 0 it means that the value for the radial wind speed is not valid; if it's 1 then the value for RWS is valid
- RWSRTStatus and HWSRTStatus: these two columns are not used by the lidar;
- HWSStatus; if it's 0 it means the value for the horizontal wind speed is not valid; if it's 1 then the value for HWS is valid;
- OverrunStatus: The overrun status is not used for any filter; it simply indicates whether or not the time of acquisition plus the time of processing match the acquisition frequency (which is by default 1 Hz).

The real time data process includes:

- LIDAR time for covering one line of sight
- Acquiring time for data reflecting back from the atmosphere
- Processing the radial wind speed data
- Processing that radial information with the previous radial data from the other line of sight to compute horizontal wind speed and direction

If the above process takes more than 1s at 1Hz, a "0" value is provided for the overrun status as it is no longer at 1 Hz. resolution. The data will still be taken into account to compute 10min data, where it is still valid.

N.B.! It's important to note:

The 10 min mean and standard deviation of the horizontal wind speed is based only on half of the 10 min period. This can be checked with the following query in mysql:

Example Queries	<pre>SELECT TIMESTAMP, AVG(HWS), AVG(RWS) FROM walney_public.windiris_fast2 WHERE TIMESTAMP BETWEEN '2013-03-20 12:00:00' AND '2013-03-20 12:09:59' AND lineofsight = 0 AND distance = 267 GROUP BY distance, lineofsight</pre>	<pre>SELECT NAME, HWS, RWS FROM walney_public.iris_meanstdv3_b0 WHERE NAME = 201303201300 AND distance = 267</pre> <p>Note the 1 hour time difference in the where clause (201303201300)</p>
Results	<pre>HWS = 40.13093340 RWS = 7.988000137</pre>	<pre>HWS = 40.13093340 RWS = 7.988000137</pre>

## Time stamp

The time stamp on the data in the tables corresponds to:

- For tables iris\_meanstdv3\_b0 and iris\_meanstdv3\_b1:  
 UTC +0h in the column D\_T  
 UTC+1h in the column Name

## Available data

**Table 5.22 Minimum and maximum time stamp in the tables with nacelle lidar data (note that the period identified below corresponds to several different settings of the lidar)**

Table name	Start	End	Time corresponds to
iris_meanstdv3_b0	12-03-2013 12:41	21-02-2014 00:30	UTC+1h
iris_meanstdv3_b1	12-03-2013 12:41	21-02-2014 00:30	UTC+1h
windiris_fast2	12-03-2013 11:41:38	20-02-2014 23:36:21	UTC

**Table 6.23 Periods with missing data for each table (given in UTC+1):**

Table	Start	End	Number of days
Iris_meanstdv3_b0	18-03-2013 11:30	18-03-2013 13:30	0.08
	06-06-2013 09:00	06-06-2013 11:50	0.12
	02-07-2013 06:10	02-07-2013 23:50	0.74
	25-07-2013 08:40	25-07-2013 09:20	0.03
	29-07-2013 13:30	29-07-2013 13:50	0.01
	10-08-2013 20:50	25-09-2013 13:00	45.67
	04-11-2013 14:20	04-11-2013 14:50	0.02
	17-11-2013 11:00	17-11-2013 12:20	0.06
	12-01-2014 23:40	12-01-2014 23:50	0.01
	30-01-2014 10:20	30-01-2014 14:00	0.15
Iris_meanstdv3_b1	18-03-2013 11:30	18-03-2013 13:30	0.08
	06-06-2013 09:00	06-06-2013 11:50	0.12
	02-07-2013 06:10	02-07-2013 23:50	0.74
	25-07-2013 08:40	25-07-2013 09:20	0.03
	29-07-2013 13:30	29-07-2013 13:50	0.01
	10-08-2013 20:50	25-09-2013 13:00	45.67
	04-11-2013 14:20	04-11-2013 14:50	0.02
	17-11-2013 11:00	17-11-2013 12:20	0.06
	12-01-2014 23:40	12-01-2014 23:50	0.01
	30-01-2014 10:20	30-01-2014 14:00	0.15
	18-03-2013 11:30	18-03-2013 13:30	0.08

	06-06-2013 09:00	06-06-2013 11:50	0.12
windiris_fast2	18-03-2013 11:23:45	18-03-2013 13:36:23	0.09
	19-03-2013 09:10:55	19-03-2013 09:22:44	0.01
	06-06-2013 08:58:44	06-06-2013 11:53:45	0.12
	02-07-2013 06:03:03	02-07-2013 23:59:59	0.75
	25-07-2013 08:35:47	25-07-2013 09:32:46	0.04
	29-07-2013 13:21:07	29-07-2013 13:55:50	0.02
	10-08-2013 00:00:00	25-09-2013 13:04:46	46.54
	04-11-2013 14:14:54	04-11-2013 14:59:33	0.03
	17-11-2013 10:55:50	17-11-2013 12:22:31	0.06
	12-01-2014 23:37:25	12-01-2014 23:59:59	0.02
	22-01-2014 12:36:11	22-01-2014 12:43:10	0.00
	30-01-2014 10:14:15	30-01-2014 14:02:31	0.16

It should be noted that the indicated period of missing data means that the measurement system was not working at all. However it does not guarantee that the lidar was working properly during the rest of the time. This should be additionally checked before analyzing the data.

### Calibrations

The direction measured by the lidar does not correspond to the definition of wind direction. See nacelle lidar user manual for more information on this.

**Table 5.24 Table layout for table wind\_iris\_10min:**

Column name	Description
Name	Timestamp in UTC + 1 (or should be equal to lidar time stamp + 50min)
Timestamp	Timestamp
HWS_mean	Mean horizontal wind speed
HWS_std	Std of horizontal wind seed
HWS_min	Min of horizontal wind speed
HWS_max	Max of horizontal wind speed
Iris_dir_mean	Mean of wind direction
Iris_dir_std	Std of wind direction
Iris_dir_min	Min of wind direction
Iris_dir_max	Max of wind direction
RWS_mean	Mean of RWS
RWS_std	Standard deviation of RWS
RWS_min	Min of RWS

RWS_max	Max of RWS
RWSD_mean	Mean of RWSD
RWSD_std	Std of RWSD
RWSD_min	Min of RWSD
RWSD_max	Max of RWSD
CNR_mean	Mean of CNR
CNR_std	Std of CNR
CNR_min	Min of CNR
CNR_max	Max of CNR
Tilt_mean	Mean of tilt
Tilt_std	Std of tilt
Tilt_min	Min of tilt
Tilt_max	Max of tilt
Roll_mean	Mean of roll
Roll_std	Std of roll
Roll_min	Min of roll
Roll_max	Max of roll
RWSStatus	Mean of RWSStatus
RWSRTStatus	Mean of RWSRTStatus
OverrunStatus	Mean of OverrunStatus
HWSStatus	Mean of HWSStatus
HWSRTStatus	Mean of HWSRTStatus
Count	Number of samples within a 10min period

### Wave Buoy Measurements

The wave buoy is situated around 40m away from the D01 turbine. The data from the wave buoy measurements are placed in six different tables in the database.

- 1) Wavecurrents (30 min. statistical data)

**Table 5.25 Columns and units in the table "wavecurrents"**

Column name	Units	Comments
Name	yyyymmddhhmm	Timestamp
Latitude	[deg]	Coordinates
Longitude	[deg]	Coordinates
Depth		Wave depth

Wtemp		Water temperature
Pressure	[?]	This column is practically redundant; all values are 0
Sound_spd		Speed of sound
Velocity1		Velocity at surface
Dir1		
Velocity2		Velocity below surface
Dir2		
Velocity l, l = 3..50		Velocities below surface at different heights.
Dir l, l = 3..50		

2) Table Wave Statistics (Wavedata) (30 min. statistical data)

**Table 5.26 Columns and units in table “wavedata”**

Column name	Units	Comments
Name	Yyyymmddhhmm	Timestamp
Location	DDMM.MMM/DDMM.MMM	Coordinates(*see example below)
Zcross	[-]	Number of zero crossings
Havg	[m]	Average wave height
Tz	[s]	Mean spectral period
Hmax	[m]	Maximum wave height
Hsig	[m]	Significant wave height. The average is calculated based on 1/3 of the highest wave heights registered.
Tsig	[s]	Significant wave period
H10	[m]	The average height of the highest tenth of the waves
T10	[s]	Wave period for H10
Meanperiod	[s]	Mean wave period
Peakperiod	[s]	Peak wave period; based on the frequency at which the wave spectrum has its maximum value
Tp5	[s]	Peak wave period (based on spectral moments)
Hm0	[m]	Significant wave height;

		determined based on the spectral analysis;
MeanMagDir	[deg]	Mean magnetic direction; Indicates the direction from which the wave is coming;
Meanspread	[deg]	Overall direction spreading width
MeanTrueDir	[deg]	Values are either -10 or 0 – probably means non-valid measurements
Te	[s]	Wave energy period
Steepness	[-]	Wave steepness; calculated by dividing the wave height by the wave length

\*Example: 5405.7449N 00313.6170W – 54<sup>0</sup> 05.7449’N 3<sup>0</sup> 13.6170’W

3) Tables wavedata\_30minbuoy1 and wavedata\_30minbuoy2 (30 min. statistical data)

**Table 5.27 Columns and units in tables “wavedata\_30minbuoy1” and “wavedata\_30minbuoy2”**

Column name	Units	Comments
Name	Yyyymmddhhmm	Timestamp
Freqindex	[-]	
Frequency	[Hz]	
SpecDensity	[M <sup>2</sup> /Hz]	Spectral density
Wave_dir	[deg]	Mean wave direction
Width	[deg]	Spreading width

4) Tables wavedata\_rundefbuoy1 and wavedata\_rundefbuoy2

**Table 5.28 Columns and units in tables “wavedata\_rundefbuoy1” and “wavedata\_rundefbuoy2”**

Column name	Units	Comments
Name	Yyyymmddhhmm	Timestamp
Start_dt		

Stop_dt		
Mean_dir		
Mean_width		

### Time stamp

The time stamp on the data in the tables corresponds to:

UTC + 1h

### Available data

**Table 7.29 Minimum and maximum time stamp in the tables**

Table name	Start	End
Wavecurrents	01-03-2012 06:20	30-09-2013 08:21
wavedata	01-03-2012 07:00	30-09-2013 08:00
Wavedata_30minbuoy1	01-08-2011 10:00	19-12-2011 21:00
Wavedata_30minbuoy2	01-08-2011 10:00	17-12-2011 21:00
Wavedata_rundefbuoy1	01-08-2011 10:00	19-12-2011 21:00
Wavedata_rundefbuoy2	01-08-2011 10:00	17-12-2011 21:00

The above description of all tables completes the description of the measurement database which is the main deliverable of the project and has been successfully completed.

## 6.0 Wind and SCADA Measurements on the Instrumented Turbine

In order to evaluate the wind measurements made from different sensors placed on top of the nacelle of wind turbine D01, the database readings as described in the last chapter for wind measurements were simultaneously processed. Wind speed measurements were provided by two cup anemometers – one of them provided by Siemens, the other one – by DTU. The two cup anemometers were there during the entire duration of the project. Additionally a nacelle-based lidar (wind Iris) was placed on top of the turbine in the period from 12-03-2013 to 22-02-2014. It was used to measure wind speed and direction at 5 different ranges in front of the turbine. There was also a relative humidity sensor, a pressure sensor and a temperature sensor. A simplified representation of the different sensors and their connection is given in Fig.6.1.

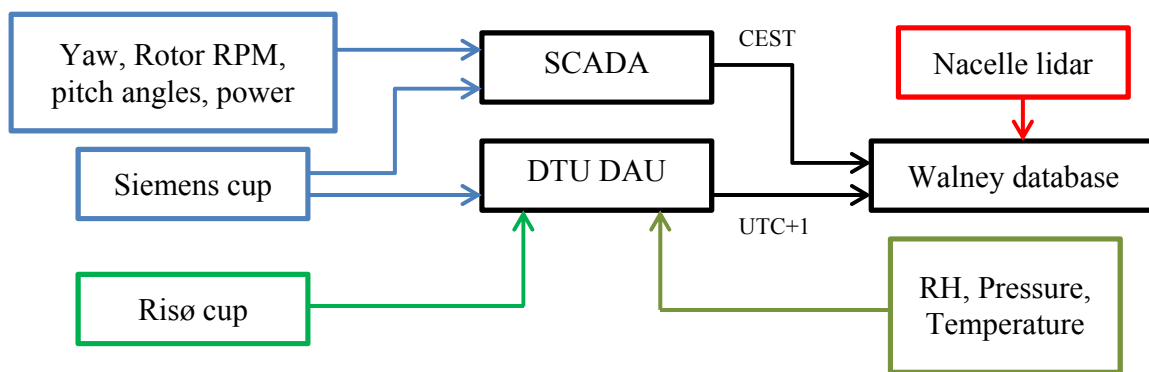


Figure 6.1 Diagram of instruments mounted on the nacelle of D01 and their connection to the measurement systems

### 6.1 Cup anemometers and nacelle-based lidar

There were two cup anemometers mounted on top of the nacelle of turbine D01. One of them was supplied by Siemens and was used for wind turbine control. Its measurements were recorded through the SCADA system and DTU system. The other one – a Thies cup – was provided by DTU and the wind speed data was recorded via DTU measurement system. All sensors on top of the nacelle provided by DTU have been calibrated and they are listed in Table 6.11. The data from all these sensors (stored in walney\_public.calmeans) covers a period of almost three years: from 12-06-2012 to 15-04-2015.

Table 6.1 List of sensors used to measure wind speed, relative humidity, pressure and temperature

Sensor:	Measurand:	Serial number	Calibration date
Thies cup anemometer	Wind speed	2624	15-06-2012
Pt100	Temperature	0743	02-02-2012
Vaisala HMP155	Relative humidity Atmospheric pressure	2646	06-09-2011



The nacelle lidar data covers a period of approximately 1 year: from 12-03-2013 to 21-02-2014. It measures wind speed and direction at 5 different ranges: 214m, 267m, 321m, 374m and 428m. It should be noted that the direction measured by the lidar is not the actual wind direction but can be interpreted as the yaw misalignment of the wind turbine. It is possible however to obtain the wind direction from those measurements.

In order to verify the wind speed measurements a few plots will be presented below showing the correlation between the two cups and between the lidar and the Thies cup.

The horizontal wind speed measured by the lidar is calculated from the ten minute averages of the radial velocities. First the longitudinal component  $V_l$  and the transverse component  $V_t$  are calculated:

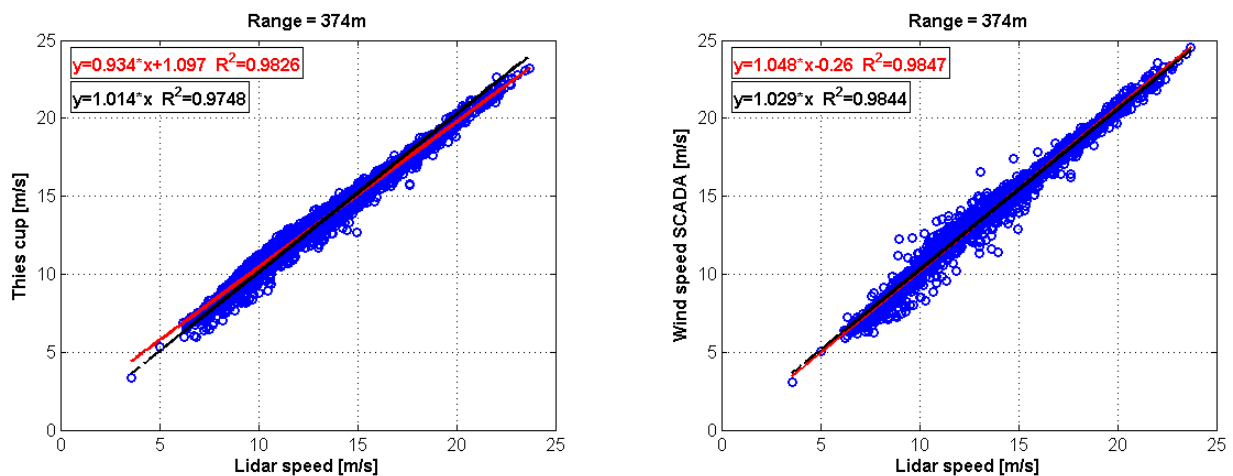
$$V_l = \frac{rws_0 + rws_1}{2 * \cos(\phi)}$$

$$V_t = \frac{rws_0 - rws_1}{2 * \sin(\phi)}$$

...where  $\phi$  is the half-opening angle of the lidar,  $15^\circ$ .  $rws_0$  and  $rws_1$  are the 10min averages of the radial velocities measured by beam 0 and beam 1 respectively. The horizontal wind speed  $V_h$  is obtained from the following formula:

$$V_h = \sqrt{V_l^2 + V_t^2}$$

In order to compare the measurements from the two cups and the lidar the time period from 01-08-2013 00:00 to 28-02-2014 23:50 was chosen. To make sure the data quality was good some additional filters were applied: rotor rotational speed > 0; pitch angle < 30; difference in yaw measurements < 5deg; standard deviation of lidar horizontal wind speed < 5m/s and yaw angle between 130 and 190. After the filtering, about 200 hours of data remain. The linear regression plots are presented in Figure .



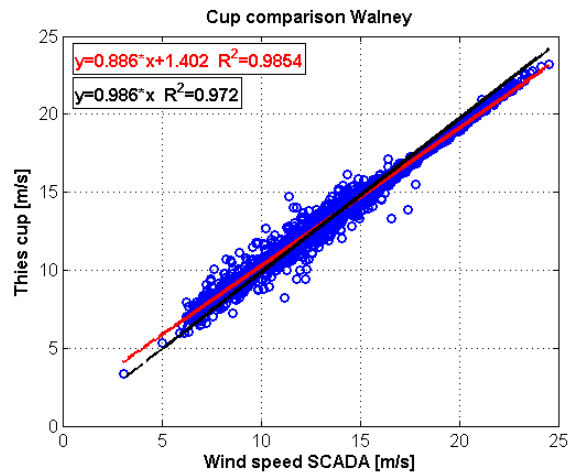


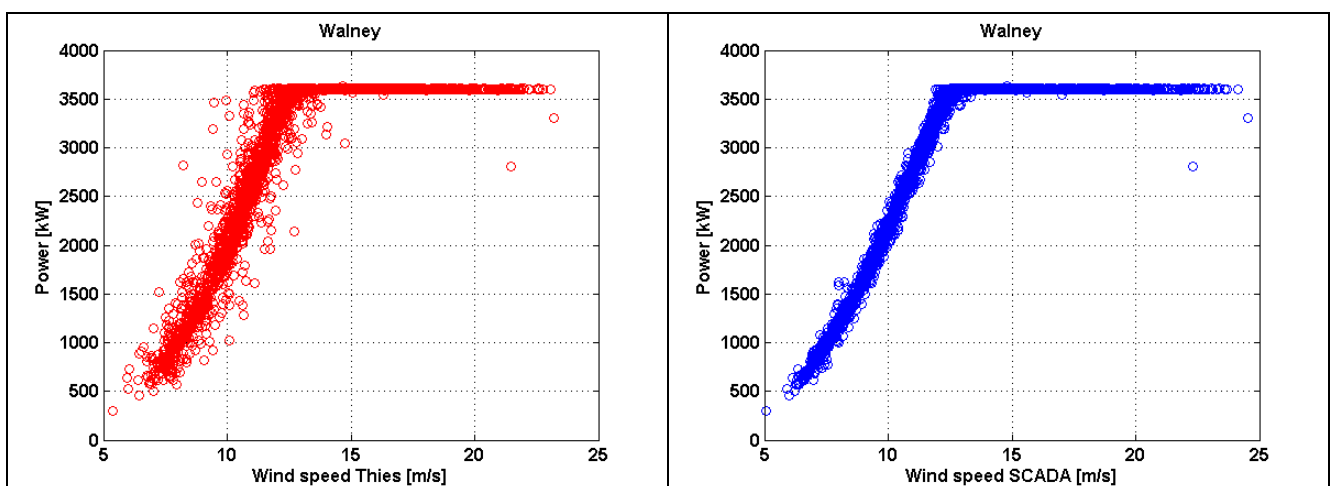
Figure 6.2 Comparison between the three different speed sensors

The Lidar measurements can be used also for obtaining a nacelle transfer function for any of the cup anemometers on the nacelle.

## 6.2 SCADA measurements

Within the frame of the Walney project, SCADA data was collected from six different turbines: C01, C02, D01, D02, E01 and E02. This data includes turbine yaw, rotor rotational speed, pitch angles of all blades, wind speed and power output.

The scada data combined with the wind speed data can be used for example to obtain the power curve of D01. Three different power curves – obtained with the two cups and the nacelle lidar are presented in Figure . The data was filtered in the same way as it was specified in the previous subsection.



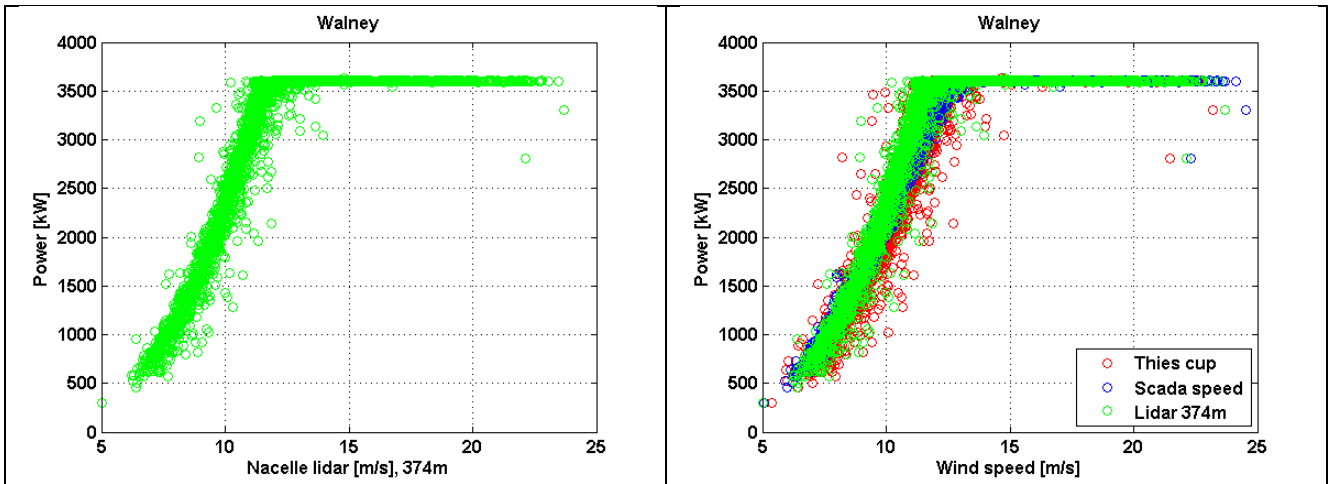


Figure 6.3 Power curves for D01 obtained with three different wind speed sensors.

Besides the SCADA data and lidar data, the database also includes load measurements on the turbine itself (tower, blades and gearbox shafts) and the turbine foundation, measurements from a wave buoy which was deployed in the waters close to D01. All these systems were operational during different stages of the project. In Figure a quick overview is given of the periods covered by the different systems. More details can be found in Section 5.

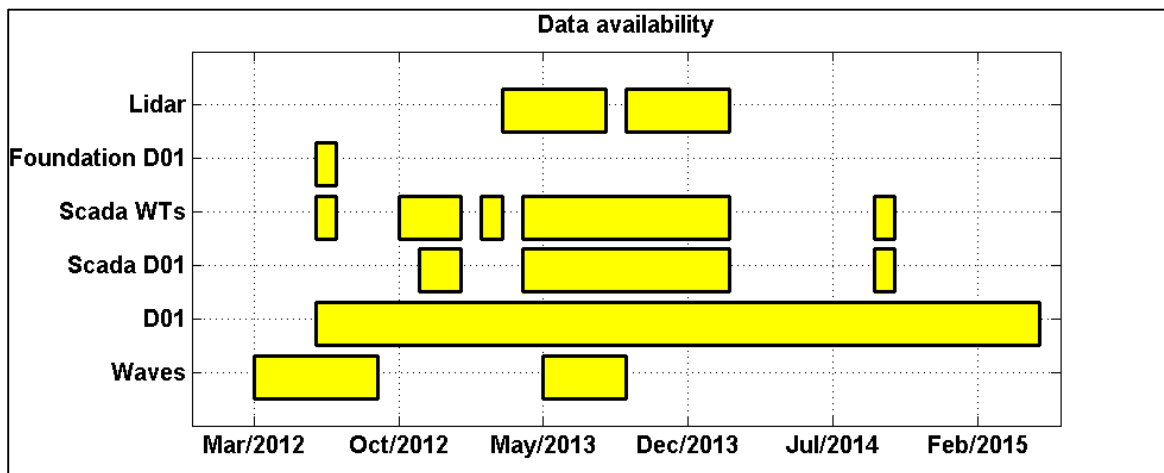


Figure 6.4 Data from the different systems available in the database

## 7.0 Validation of Environmental Models and Load Simulations with Measurements

Before the comparison of HAWC2 simulated loads with measurements, a calibration of the raw data from the strain gauges of the instrumented wind turbine is required. Due to imbalances in the bridge circuit, the output data from the acquisition device  $\varepsilon_{out}$  always includes an offset  $\varepsilon_{offset}$ . The offset is calculated by performing a yaw test, where the Rotor-Nacelle Assembly (RNA) is rotated 360 degrees around its vertical axis. The following equations 7.1 to 7.4 are taken from Ref. [2]. The bending strain is given by (Eq.7.1):

$$\varepsilon_B = \varepsilon_{out} - \varepsilon_{off.yawTest} \quad (7.1)$$

The bending strain is transformed to bending moment through (Eq.7.2):

$$M_B = \frac{EI}{R} \varepsilon_B \quad (7.2)$$

Where  $EI$  is the bending modulus of the support structure and  $R$  is the radius of the monopile where the strain gauges are mounted. The calculated bending moment is transformed to the rotated system that follows the wind turbine.

$$M_{x,rot} = M_x \cos(a-y) - M_y \sin(a-y) \quad (7.3)$$

$$M_{y,rot} = M_x \sin(a-y) + M_y \cos(a-y) \quad (7.4)$$

Where  $a$  is the angle between the strain gauge position and the north orientation and  $y$  is the yaw angle at each time step.

### Soil Model

For the lateral loading of the monopile, the commonly used p-y curve method is employed, where the soil stiffness is modeled by distributed nonlinear springs, as shown in Figure 7.1a. The soil spring forces are depth dependent. Based on DNV-OS-J101 2007 [3] standard, for every deflection  $y$  there is a lateral resistance  $p$  per unit length of pile according to the type of the soil (sand or clay). The p-y curve can be generated from (Eq. 7.5) for sand and (Eq. 7.6) for clay:

$$p = Ap_u \tanh\left(\frac{kX}{Ap_u} y\right) \quad - (7.5)$$

$$p = \left\{ \begin{array}{ll} \frac{p_u}{2} \left(\frac{y}{y_c}\right)^{1/3} & \text{for } y \leq 3y_c \\ 0.72 p_u \left(1 - \left(1 - \frac{X}{X_R}\right) \frac{y - 3y_c}{12y_c}\right) & \text{for } 3y_c < y \leq 15y_c \\ 0.72 p_u \frac{X}{X_R} & \text{for } y > 15y_c \end{array} \right\} \quad - (7.5)$$

Where  $p_u$  is the static ultimate lateral resistance per unit length,  $X$  is the depth below soil surface,  $A$  is a factor with value 0.9 for cyclic loading,  $k$  is the initial modulus of subgrade reaction that depends on the friction angle  $\varphi$ ,  $y_c = 2.5\varepsilon_c D$ , in which  $D$  is the pile diameter and  $\varepsilon_c$  is the strain which occurs at one-

half of the maximum stress and  $X_R$  is a transition depth. The soil characteristics are based on site measurements.

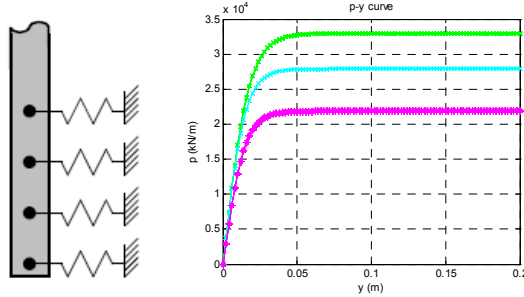


Figure 7.1: a) distributed springs model. b) Soil model, p-y curve for different depth values

### Site Wind Turbulence Intensity

The wind turbulence intensity is calculated by the standard deviation of the horizontal wind speed measured at the hub height  $z_{hub}$  divided by the measured mean wind speed  $U_{hub}$  (Eq. 7.7).

$$I = \frac{\sigma}{U_{hub}} \quad (7.6)$$

For the calculation of the turbulence intensity to be used in loads simulations, the 90<sup>th</sup> percentile of the standard deviation is used according to the (IEC 61400-3 2005) (Eq. 7.8).

$$\sigma_{90} = \frac{U_{hub}}{\ln(z_{hub} / z_0)} + 1.28 \cdot 1.44 \cdot I_{15} \quad (7.7)$$

Where  $I_{15}$  is the expected turbulence intensity at 15m/s wind speed and equal to 0.16 for a wind turbine class A, as per IEC 61400-1[4] and  $z_0$  is the surface roughness length, calculated iteratively by (Eq. 7.9) as proposed by IEC 61400-3 [5] for site specific offshore wind turbine design.

$$z_0 = \frac{A_C}{g} \left[ \frac{\kappa \cdot U_{hub}}{\ln(z_{hub} / z_0)} \right]^2 \quad (7.8)$$

Where  $A_C = 0.011$  is the Charnock parameter for open sea,  $\kappa = 0.4$  is the von Karman parameter and  $g$  is the gravity acceleration.

The site measurements for the wind are nacelle anemometer readings from a cup-anemometer installed behind the rotor. This results in increased measured turbulence intensity due to the wake effects from the flow behind the blades. The yaw sector considered ensures that the instrumented wind turbine sees only undisturbed wind flow (no wake effect). An increase in the turbulence intensity can be observed for higher wind speeds, because of increased surface roughness due to wind induced waves. A fitted exponential curve to the nacelle anemometer wind measurements based on the 90<sup>th</sup> percentile of the data was used for the calculation of the turbulence intensity. The offshore turbulence conditions based on the (IEC 61400-3) wind turbine class A given by (Eq. 7.8) are also calculated. The measured turbulence intensity was found to lie close to the wind class A and since this is a measurement from the nacelle anemometer, it is considered to be conservative. The simulation of the

wind turbulence is then made based on the Mann wind turbulence model as described in the IEC 61400-1.

### Wind Turbine Model set-up

The model for the 3.6MW wind turbine is built by down-scaling the NREL 5MW reference offshore wind turbine, applying the similarity rules. Modifications in the mass and stiffness distribution of the blade and support structure have then been made to the derived downscaled model in order to match the natural frequencies and the total mass given by the manufacturer. Table 7.1 and 7.2 depicts the differences observed between the model characteristics and the real turbine [2].

**Table 7.8: Difference in the natural frequencies between model and real wind turbine**

Natural Frequencies	Percentage difference
1 <sup>st</sup> flapwise bending	0.13 %
1 <sup>st</sup> edgewise bending	0.9 %
2 <sup>nd</sup> flapwise bending	4.25 %
2 <sup>nd</sup> edgewise bending	19.15 %
1 <sup>st</sup> tower along wind	0.19 %
1 <sup>st</sup> tower across wind	0.9 %
1 <sup>st</sup> symmetric flap	2.51 %

**Table 7.9: Difference in the mass properties between model and real wind turbine**

Mass characteristics	Percentage difference
Blade mass	0.16 %
Blade center of gravity	0.08 %
Tower top mass	0.24 %

The modal characteristics from Tables 7.1 and 7.2 seem to be within acceptable limits and the turbine model reasonably represents the actual wind turbine on site so that the simulation results can be considered comparable.

The waves on the offshore site are simulated based on site measurements of significant wave height and peak crossing period, from which a JONSWAP spectral model is derived. The variable speed generator and symmetric blade pitch control of the wind turbine is modeled through a proportional integral-controller (PI). The operation of the wind turbine is separated in three regions, depending on the wind speed as shown in (Fig. 3). For the verification of the controller behavior, the power curve resulting from the simulations is matched against the power curve provided by the manufacturer.

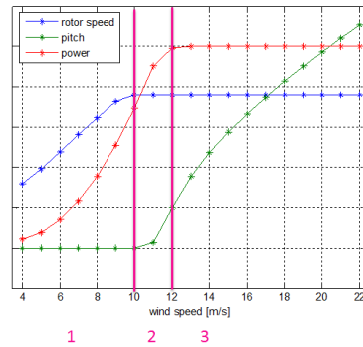


Figure 7.2 : Modeled wind turbine Performance

### Nacelle LIDAR

A nacelle mounted LIDAR is installed on the wind turbine, to measure the upstream wind flow. The wind speed measured by the two beams is combined by the following equation to construct the wind seen by the turbine.  $V_l$  and  $V_r$  are the radial wind speed measured by each beam and  $\alpha_{lidar}=30^\circ$  the angle between the two beams.

$$V_h = \sqrt{\left(\frac{V_l + V_r}{2 \cos(\alpha_{lidar})}\right)^2 + \left(\frac{V_l - V_r}{2 \sin(\alpha_{lidar})}\right)^2} \quad -(7.10)$$

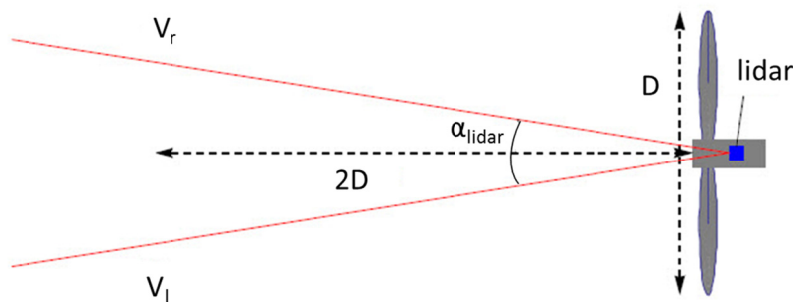
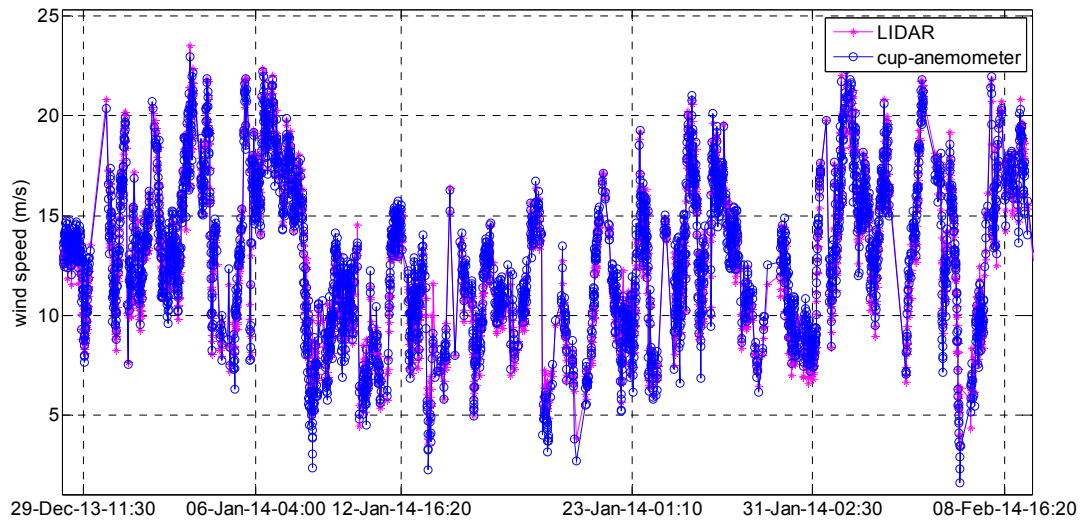


Figure 7.3 Schematic View of the LIDAR

For the synchronization of the nacelle mounted LIDAR the mean values of the 10min mean wind speed over a period of time measured by the DTU nacelle cup-anemometer and the LIDAR are plotted against each other in Fig. 7.4. A time lag of 1-hour, where the LIDAR is following, has been observed.



**Figure 7.4:** Comparison of averaged wind speed measurements from the LIDAR with the cup anemometer

### Wave Measurement Analysis

A buoy installed close to the wind turbine on the site is measuring the surface elevation and the wave direction in a time interval of 30 minutes. The time series of the surface elevation are used to estimate the wave properties, like the wave spectrum, the significant wave height  $H_s$  and the peak period  $T_p$ . Figure 7.5 presents  $H_s$  and  $T_p$  as a function of the mean wind speed as measured by the buoy.



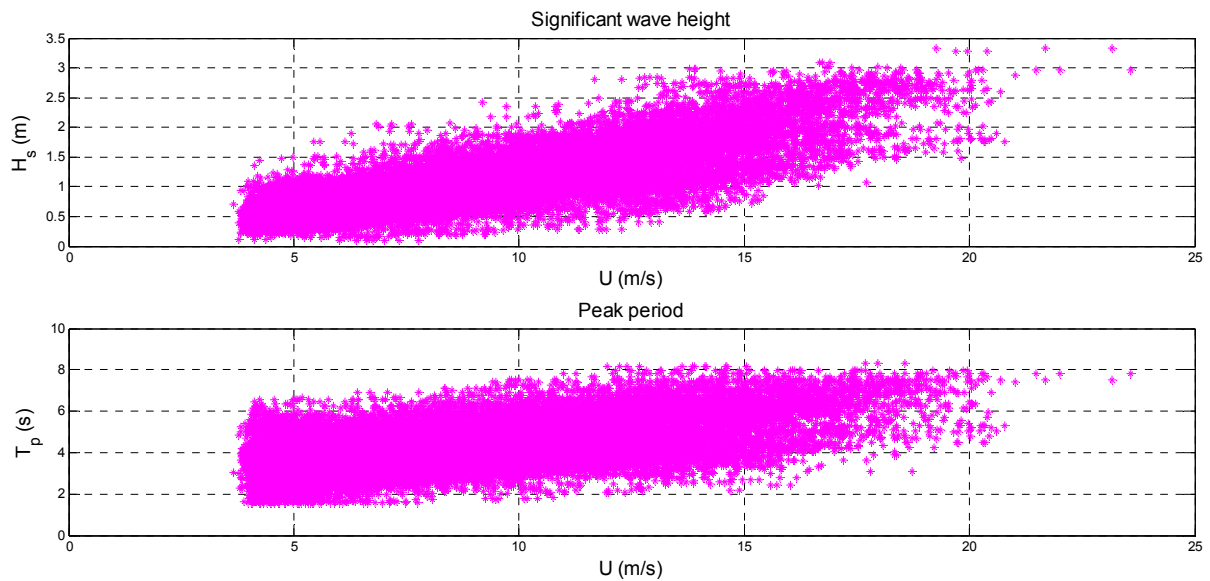


Figure 7.5: Scatter plot of measured significant wave height and peak period

A Fast Fourier Transformation (FFT) fit to the measured data results in the wave spectrum, from where the peak frequency  $f_0$  can be identified as the frequency that corresponds to the maximum wave energy. The following figure presents the power spectrum of a 30min wave time series, along with the fitted JONSWAP spectrum [5].

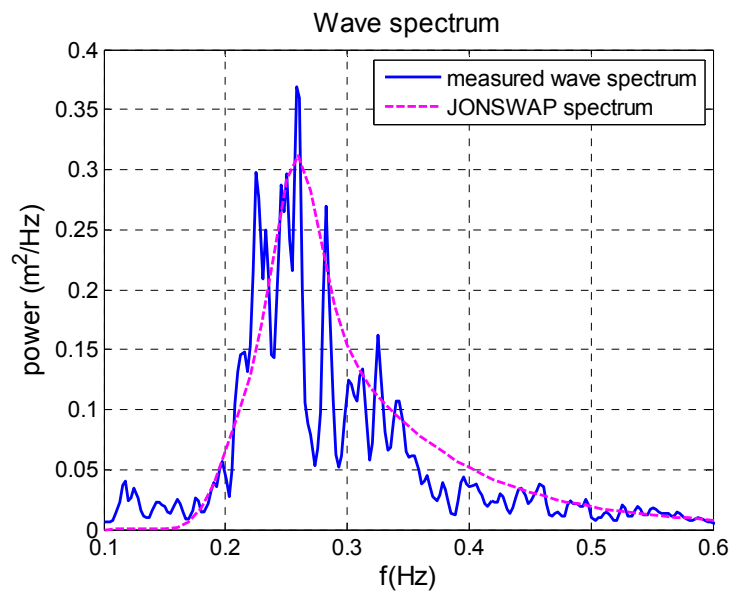
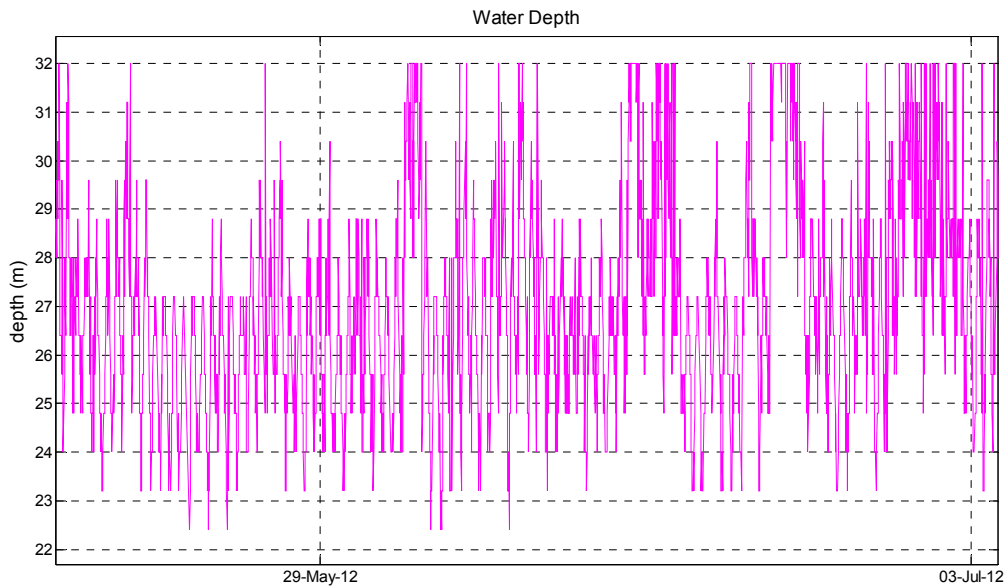


Figure 7.6: Measured power spectral density of wave height

The buoy also measures the velocity and the direction of subsurface current every 0.8m below the water surface till the seabed. The position of the sea bed can be identified as the position that gives an erroneous current speed value, which indicates the water depth and is used to study the effects of tide. Figure 7.7 presents the variations in the water depth over a period of 2 months. The mean water depth is 27m and the tidal variation is  $\pm 5\text{m}$  around that.



**Figure 7.7: Measured variations in water depth due to Tidal changes**

The uncertainty on the wave direction measured by the buoy is identified by comparing the mean wave direction with the peak wave direction (i.e. the direction that results in the highest energy from the directional spectrum). The Fig. 7.8 compares the peak and the mean wave direction from the buoy, where on the y axis the mean wave direction measured by the buoy and on the x the peak direction are presented. This shows that the wave direction has an uncertainty of around  $\pm 30^\circ$  (93% confidence interval). Therefore, for the construction of the wave rose the directions are separated in 12 bins of  $30^\circ$  each.

For the estimation of the short term joint wind-wave distribution the conditional wave probability (Weibull distribution) is combined with the wind probability. Figure 7.9 presents the contour surface of the short-term joint distribution. The average wind speed is 9m/s. The lower estimated wind from the joint wind-wave distribution than the expected site conditions (9.6m/s) is due to the short measurement period of six months, which might not be representative of the site (wind index).

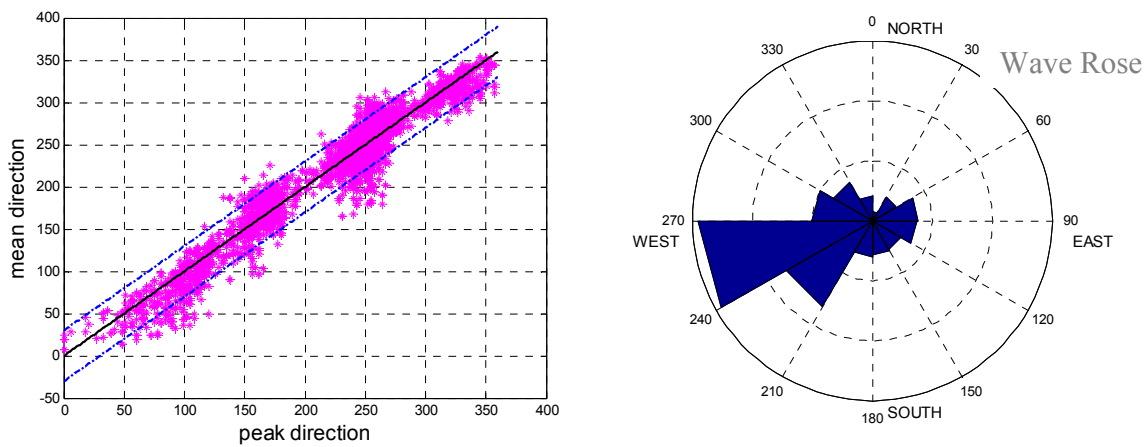


Figure 7.8: Measured direction of the waves

Based on the histogram of the wind and wave direction, it was found that a two parameter extreme value distribution described best the probability of wind/wave misalignment. From the mode of the two distributions (Figures 7.10a, 7.10b) it can be observed that the main wind and wave directions have a difference of nearly  $10^{\circ}$ , with the expected wind/wave misalignment from the mean of the fitted distribution to be  $9.2^{\circ}$ .

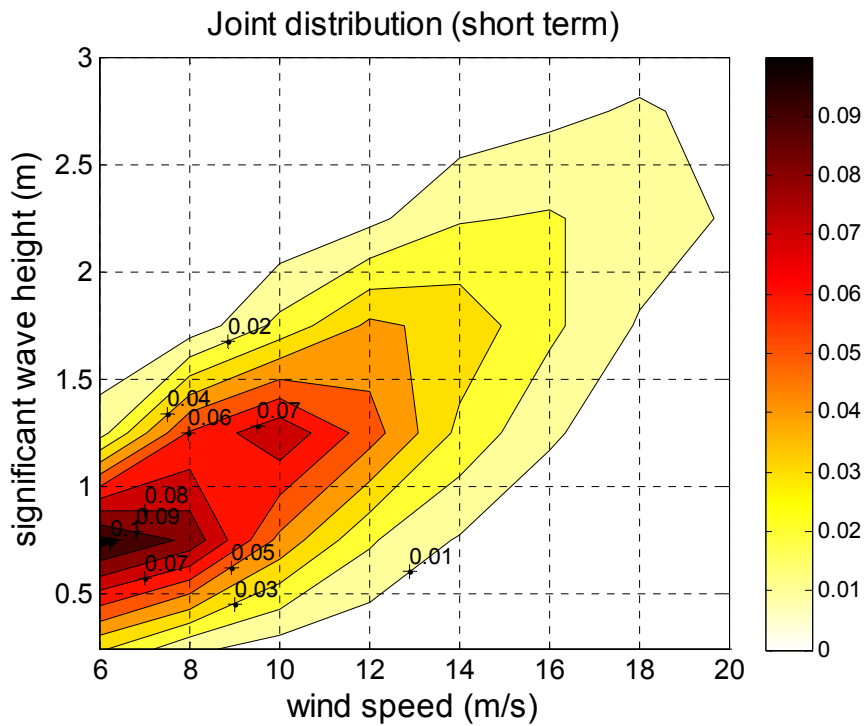
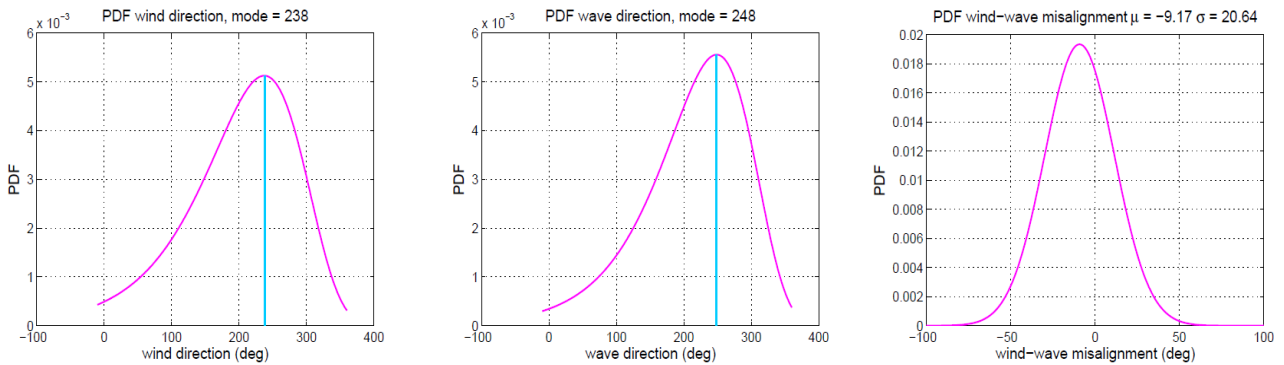


Figure 7.9: Probabilistic return contours of the significant wave height



**Figure 7.10: Probability distributions of wind, wave directions and their misalignment**

The measured waves were also used to quantify any nonlinear wave characteristics since usually irregular waves are modeled as a linear process. However nonlinear irregular wave models have been developed and the measured waves can be used to validate these nonlinear wave models.

A nonlinear wave was measured on the site wherein the measured wave significant height was 2.67m, but a sharp peak of 4.06m was seen at 484 seconds as seen in Fig. 7.11a [6]. It can also be seen that the wave troughs are very shallow; seldom below -1.8m. The high peak at 484 seconds and the shallow troughs in the vicinity of the peak are clear indications of a nonlinear process. Figure 7.11b compares the measured wave time series to a linear random wave and to a second order random nonlinear wave obtained by fitting the first 4 moments of the process to the measured wave. It can be seen that the second order wave matches the measured peak crest at 484 seconds very well, but it does not have identical shallow troughs, a feature that requires even higher stochastic moments. However the linear wave neither reaches the peak nor has shallow troughs near the vicinity of the extreme crest.

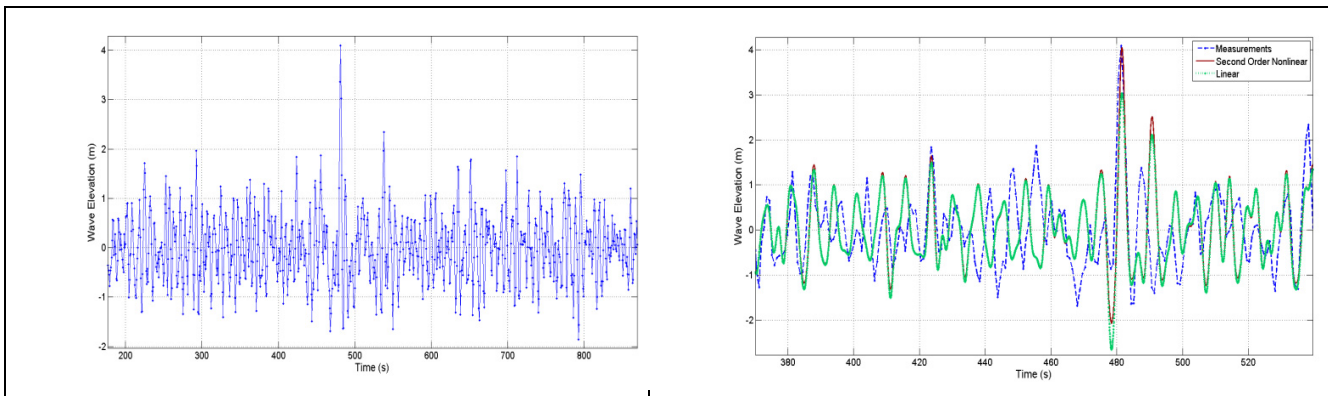


**Figure 7.11: a) Measured wave time series, b) Fitted linear and nonlinear wave model time series to measurements [6]**

### Validations of Loads on the Foundation

A comparison of the extreme values of the bending moments at two different positions along the monopile between measurements and simulations is presented in Figure 7.12 [7]. The displayed data are normalized with the simulations maximum load value at the rated wind speed. The 10min load

simulations were performed in HAWC2 based on DLC 1.1(IEC 61400-1 2005) with 12 different turbulent seeds per mean wind speed. A yaw sector where the wind turbine sees undisturbed flow was considered for this analysis. Near the rated wind speed, the maximum loads for the  $M_x$  moment are observed. At higher mean wind speeds the blades pitch, thus decreasing the peak loads acting on the wind turbine foundation.

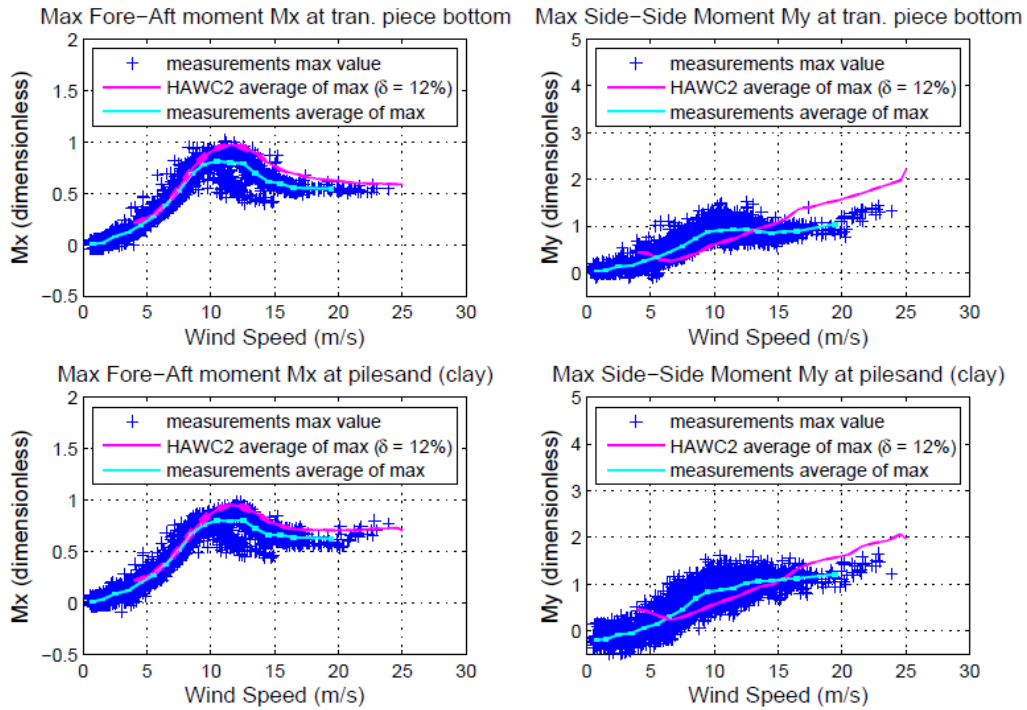


**Figure 7.12: Validation of simulated extreme loads on the monopile with measurements**

The fatigue damage of the structure is determined by using SN-curves and applying the Miner's rule to compute the damage equivalent loads as obtained from HAWC2 simulations and site measurements. For every mean wind speed, 1 hour of simulation data was used to compute the damage equivalent load. The 1Hz equivalent load associated to a number of equivalent cycles ( $n_{eq}$ ) equal to the total simulation time for every wind speed is given by (Eq. 7.11).

$$S_{eq} = \left( \frac{\sum_{i=1}^M N_i S_i^m}{n_{eq}} \right)^{1/m} \quad (7.11)$$

where  $N$  is the number of cycles related to load  $S$  and  $m$  is the Wöhler exponent depending on the material ( $m = 4$  for steel support structures). The number of cycles for a given stress range is calculated with the technique of Rainflow counting. The lifetime equivalent load  $S_{Leq}$  can be extrapolated summing up the fatigue load spectra for all the load cases and using the Weibull wind probability distribution as weighting function, as in:

$$S_{Leq} = \left( \frac{\int S_{eq}(u)^m Np(u) n_T du}{n_T} \right)^{1/m} \quad (7.12)$$

where  $p(u)$  is the wind probability distribution and  $n_T$  is the expected lifetime of the wind turbine, which is taken to be 20 years.

Considering wind speed measurements of 7 months from the site, a Weibull distribution is fitted to the data with scale and shape parameters  $\alpha = 10.69\text{m/s}$  and  $\beta = 1.98$  respectively. The shape parameter  $\beta$  is obtained by solving iteratively Eq. 7.13.

$$\frac{\sum_{i=1}^n (U_i^\beta \ln U_i)}{\sum_{i=1}^n U_i^\beta} - \frac{1}{\beta} - \frac{1}{n} \sum_{i=1}^n \ln U_i = 0 \quad (7.13)$$

and  $\alpha$  is obtained as

$$\alpha = \left( \frac{1}{n} \sum_{i=1}^n U_i^\beta \right)^{1/\beta} \quad (7.14)$$

The resulting Weibull probability distribution function is shown in Figure and is given by Eq. 7.15.

$$f(U; \beta, \alpha) = \frac{\beta U^{\beta-1}}{\alpha^\beta} \exp \left[ - \left( \frac{U}{\alpha} \right)^\beta \right] \quad (7.15)$$

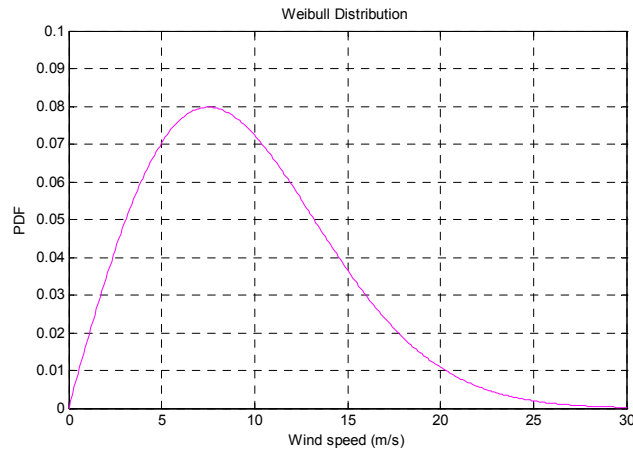


**Figure 7.13: Wind probability distribution function Weibull**

The turbulence intensity is corrected for the wake turbulence based on mean wind speed measurements and by using the Sten Frandsen wake model as shown in Fig. 7.14 below.

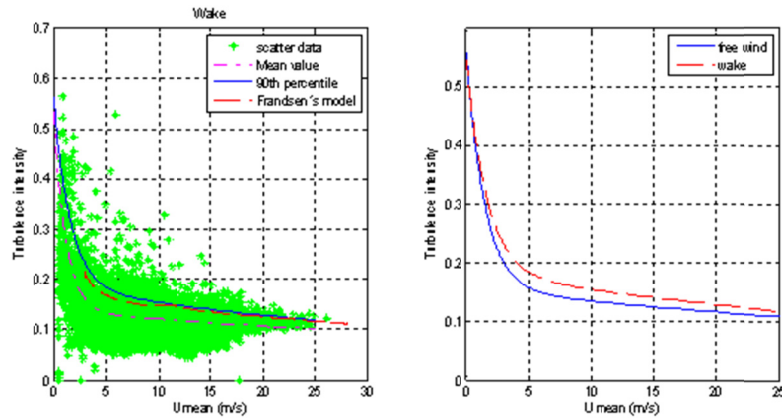


**Figure 7.14: Wind turbulence intensity as evaluated using the nacelle anemometer showing a wide scatter**

Using Eq. (11), the 1Hz, damage equivalent loads are computed for the fore-aft and side-side moments at the mud level. The mean of the simulated damage equivalent loads is compared with the mean of the measured damage equivalent loads.

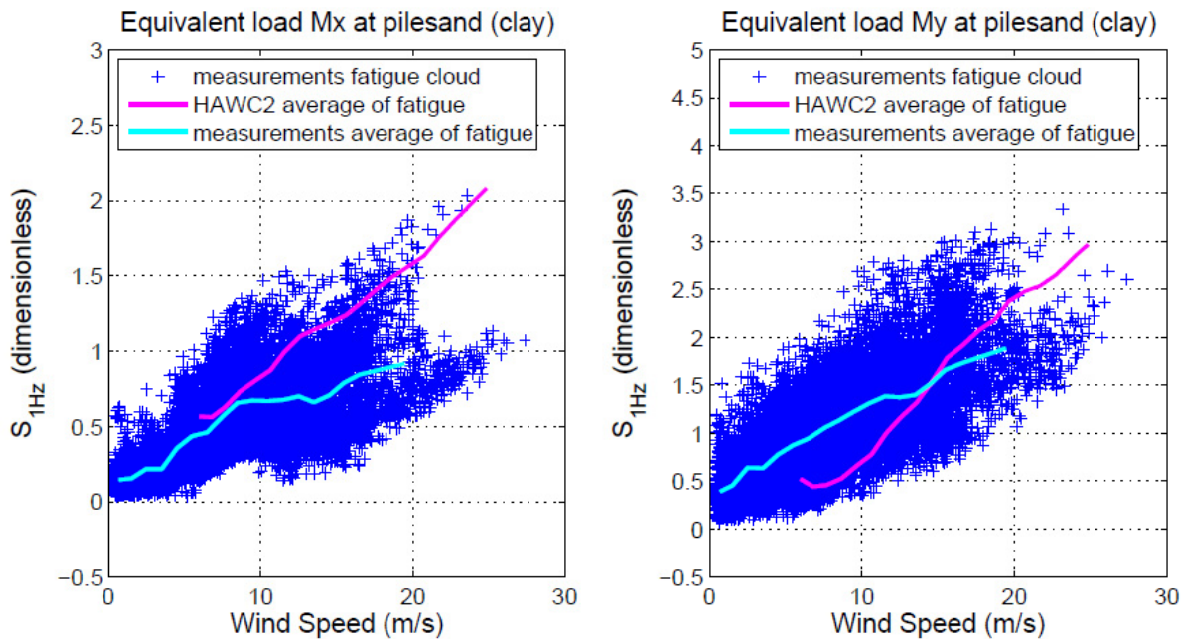


**Figure 7.15: Validation of damage equivalent loads at the mud level**

As seen from Fig. 7.15, the mean of the measurements and the mean of simulations follow the same trend at the mud level, with the simulated loads in general higher than the measured loads above rated wind speed. The differences in the comparisons are mostly due to the different aerodynamic parameters

used in the blade model and the errors in the measured wind turbulence. More details are given in Ref [1]

The Walney wind farm experienced many days of high mean wind speeds during the measurement period spanning 2011-2014. The number of shutdowns suffered by the turbines from which measurements were available was monitored as such information is rarely available publically and is important for the design of wind turbine components and reliability. The frequency of shutdowns was based on measurements on 5 turbines where SCADA information was collected [8] and it was seen that the number of shutdowns for each of the 5 turbines were closely related. The mean shutdowns per year per turbine was determined as 65, with a std. deviation of 11, where more than 50% of the shutdowns occur at high mean wind speeds in excess of 21m/s. This can of course be turbine controller dependent.

Further the site specific annual mean wind speed distribution as given in Chapter 3, table 3.1 varies significantly in various sectors and for the measurement wind turbine D01, the site specific annual mean wind speed was fit with a Weibull distribution exponent of 2.6. However the short term analysis in Fig. 8.13 shows that the annual wind speed follows a near Raleigh distribution, i.e. with exponent of 2. The comparison of the two distributions is given in Fig. 7.16 [8].

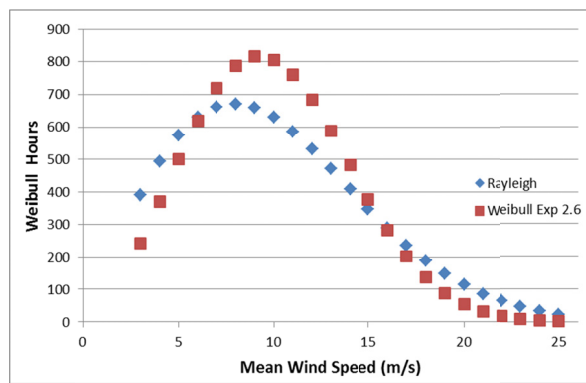


Figure 7.16: Site specific Weibull distribution compared with the standard Raleigh distribution of annual mean wind speed

The actual wind measurement on the instrumented wind turbine provide 447 hours/year where the mean wind speed was above 20 m/s, while a Rayleigh distribution provides 370 hours/year and the site specific distribution provides 120 hours. Therefore in the absence of long period of measurements, a Raleigh distribution can be used for wind turbine design and performance prediction.



## 8.0 Evaluation of Support Structure Damping

The total damping of an offshore wind turbine consists of the structural damping  $\xi_{\text{steel}}$ , the hydrodynamic damping  $\xi_{\text{hydro}}$ , the soil damping  $\xi_{\text{soil}}$  due to inner soil friction and soil-pile interaction, the passive damper on the tower top  $\xi_{\text{tower}}$ , the active damping from the control system during operation  $\xi_{\text{control}}$  and the aerodynamic damping  $\xi_{\text{aero}}$  (Equation 8.1). In standstill conditions when the blades are pitched to their maximum pitch angle the aerodynamic damping can be neglected and the estimated damping will correspond to the additional offshore damping, namely structural, hydro, soil damping and damping from the tower damper. Herein, the additional damping of the structure was identified with the following three methods [7]: a) An exponential curve is fitted to the relative maxima of the decaying response of the tower top acceleration after the application of an impulse and the logarithmic decrement is estimated from the exponent of the function. b) The half-power bandwidth method was also applied to the data in the frequency domain to obtain another estimate of the damping. c) The damping ratio is identified from the slope of a linear curve fitted to the envelope of the auto-correlation function of the tower top acceleration under ambient excitation. The total damping of the system under normal operation is estimated with the use of the output only Enhanced Frequency Domain Decomposition (EFDD) method [7].

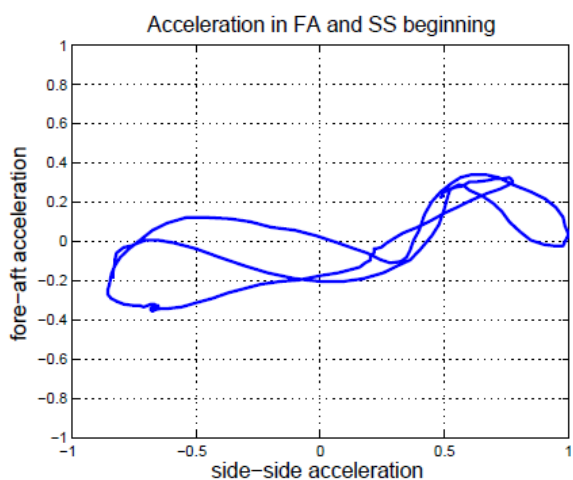
$$\xi = \xi_{\text{steel}} + \xi_{\text{tower}} + \xi_{\text{aero}} + \xi_{\text{hydro}} + \xi_{\text{soil}} + \xi_{\text{control}} \quad -(8.1)$$

During a yaw test, where the nacelle is swept slowly  $360^\circ$  around the tower axis for the calibration of the support structure strain gauges, a boat accidentally hit the tower once, acting as an impulse to the turbine. The mean wind speed during the incident was 2.5m/s and the blades were pitched out to  $82^\circ$ . The rotation of the nacelle was sufficiently slow (0.42rad/min) to assume a quasi-stationary response with no interaction with the yawing dynamics. The logarithmic decrement in tower top accelerations can be estimated from the measured time series either by fitting an exponential curve to the relative maxima (time-domain approach, exponential curve of the form  $x(t) = Ae^{-\xi\omega_n t}$ ) or with the use of the half-power bandwidth method (frequency-domain approach). The fitting of an exponential function to the relative maxima of the decaying time series for the extraction of the damping ratios from the function parameters, assumes the contribution of a single mode. Figures 8.1a and 8.1b present the tower top acceleration in the fore-aft and side-side direction at the beginning and at the end of the incident. It can be observed that the boat impact excites only the side-side vibration mode, as the boat landing is aligned with the lateral strain gauges, while the fore-aft vibration is due to wind and waves as the level of acceleration is not decreasing with time. Figure 8.1d presents the decay in the side-side direction and the fitted exponential function to the relative maxima, derived from the nonlinear least squares method.

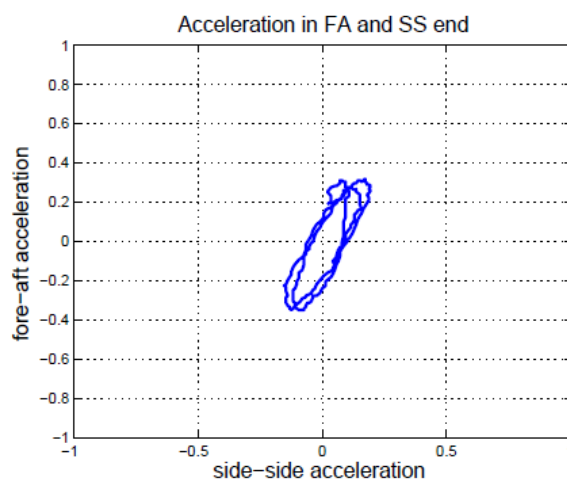
The damping ratio can be extracted from the exponent of the fitted function. The identified critical damping ratio is  $\xi = 0.019$ , which corresponds to a logarithmic decrement of 12.2% and it is in agreement with the values proposed in [9, 10]. The result is also in agreement with the overall damping of the first mode found in [11] from a measurement campaign at the Belwind wind farm. The higher damping value estimated in the present work is due to the tower damper that is not active in [11]. Therefore without a tower damper, the net damping without aerodynamics is closer to 1% critical.

A decaying response is not observed in the time series of the fore-aft acceleration in Fig. 8.1, due to the aligned boat with the side-side strain gauges when it impacts the tower, as mentioned before. The turbine is under ambient excitation in the fore-aft vibration mode, as the only forces acting are in the longitudinal direction.

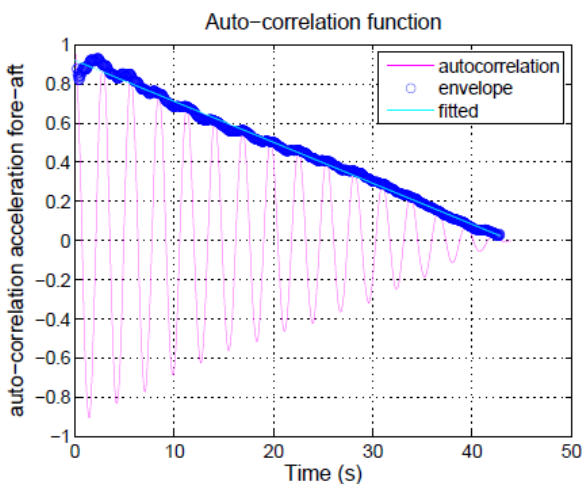
Using the enhanced frequency domain decomposition (EFDD) method [7], the same data analyzed in Fig. 8.1 was re-done to obtain the damping coefficient and the logarithmic decrement was then determined as 0.018, which is nearly the same as that obtained using the logarithmic decrement. This was taken as a validation of the EFDD methodology and more details can be referred in [7].



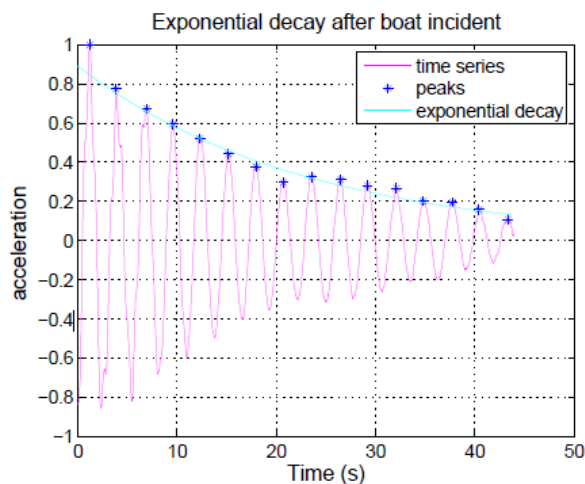
(a)



(b)



(c)



(d)

Figure 8.1: Measured decay in tower top oscillations of the wind turbine following a boat impact

The damping of the support structure was estimated from measured tower top accelerations using the EFDD method during normal operation, whereby the damping of the structure minus aerodynamics was found to be higher than normally used in load simulations, thus showing the possibility to reduce design loads. The accelerations of the support structure at 4 different tower heights were used as inputs to the frequency domain decomposition technique to estimate the natural frequency and the damping ratio of the first fore-aft and side-side vibration modes of the system. In this method, based on the measured accelerations of the wind turbine tower and assuming that the external loading is unknown, the modal characteristics are estimated using the power spectra of the measured signals. The details of the method are provided in Ref. 7.

The Enhanced Frequency Domain Decomposition technique was applied in the measured accelerations of the tower. The data used for the modal parameters' identification are from the measurement period of July 2012, where the maximum observed mean wind speed was 19m/s. The results for the fore-aft and side-side modal damping identified from the measured response of the wind turbine are presented in Figure 8.2, which depicts the estimated logarithmic decrement of the net support structure damping in the fore-aft and side to side directions.

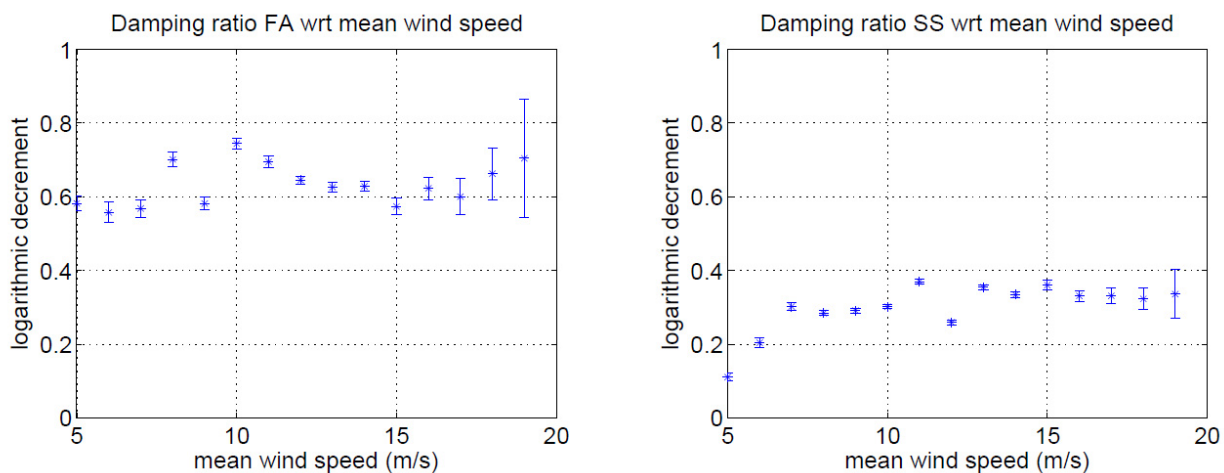


**Figure 8.2: Estimated support structure damping based on measured tower accelerations**

Based on Fig. 8.1 and 8.2, it can be concluded that the static damping capacity of the wind turbine support structure is of the order of 12% logarithmic decrement which includes all aspects of damping other than aerodynamic and the dynamic net damping including aerodynamic contributions varies between 12% to 35% in the side to side direction and 60% to 75% in the fore-aft direction. An increase of the damping ratio in the side-side direction for higher wind speeds is due to control actions and the aerodynamic damping introduced from blade pitching.

## 9.0 Key Factors affecting Support Structure Cost

In order to assess the impact of tower mode damping on the levelized cost of energy (LCOE) for an offshore wind turbine, an analysis has been made using the simplified DTU Wind Energy cost model in combination with a simplified modelling of a 3.6MW with a 107m rotor.

The DTU Wind Energy cost model is based on an economic calculation of the levelized cost and levelized energy production during the project lifetime. The cost is categorized according to the categories used in the MEGAVIND cost model:

- Capital expenditure (CAPEX)
- Development expenditure (DEPEX)
- Operational expenditure (OPEX)
- Abandonment expenditure (ABEX)

All these elements contribute to the total cost of the wind power plant during its lifetime. In the financial modelling, the discounted lifetime costs are divided with the discounted energy production. For the discounting, year 1 is used as basis and a weighted average cost of capital (WACC) are applied in combination with an assumed inflation.

The annual energy production (AEP) is based on a generic power curve calculation, assuming a maximum aerodynamic rotor efficiency below rated power, and then afterwards applying losses for the various elements in the drive train (gear, generator, converter).

For this analysis, the abandonment expenditure has been neglected, and the development expenditure has been assumed to consist of a lump sum placed in year 1. The operational expenditure has been assumed to be dependent on the energy production and a cost for each produced kWh has been applied, timed consistently with the production.

For the capital expenditure modelling a combination of cost and scaling models and design models have been applied. Cost and scaling models (CSM) are well known in cost model analysis and basically they represent relations between high level turbine parameters (like diameter, rated power, hub height) and the individual component costs. Typically, such relations are based on historic data for actual turbines. These CSM relations are simple to apply but the down side is that they do not form relationship between physical input parameters (like wind/wave conditions, design related parameters or e.g. material parameters). A CSM approach has been used for most of the components in this analysis. However, a more physical cost modelling approach based on load estimations and subsequent design modelling has been applied for the rotor and for the tower designs. Thus, the material consumption – and cost – for these models depend on the design loads.

The foundation cost is an important and dominant element for the current analysis. Unfortunately, no foundation design models were available for the current analysis and a more simplified approach has been applied. The cost of the foundation has been based on a constant value for a monopile based design. The constant value changes with the cost of the tower. Thus, if a certain cost saving is seen for the tower the same cost saving is applied to the foundation cost.

The base line numbers in the cost modelling are illustrated in the Table 9.10.

**Table 9.10 Base case cost modelling parameters**

<b>Parameter</b>	<b>Value</b>
<b>Hub height</b>	90m
<b>Diameter</b>	107m
<b>Rated power</b>	3.6MW
<b>Mean wind speed</b>	9.0m/s
<b>Turbine (ex. tower/rotor) CAPEX model type</b>	Cost and scaling model
<b>Life time</b>	20years
<b>Nominal WACC</b>	0.07
<b>Inflation</b>	0.02
<b>Rotor CAPEX model type</b>	Design model
<b>Tower CAPEX model type</b>	Design model
<b>Foundation CAPEX model type</b>	1.0 M€/MW + design model for tower
<b>Electrical infrastructure CAPEX model type</b>	0.089 M€/MW
<b>Other infrastructure CAPEX model type</b>	0.1 M€/MW
<b>Assembly/Installation CAPEX model type</b>	0.22 M€/MW
<b>OPEX cost model type</b>	0.02 €/kWh
<b>DEVEX cost model type</b>	2M€ year 1
<b>ABEX cost model type</b>	0M€

The impact of changed structural damping of the fundamental tower mode has been investigated by modifying the tower loads. In order to make a general investigation and not focus only on a specific design, a range of load reduction has been analyzed. Typically, fatigue loads on a monopile substructure varies with the damping ratio  $\xi$  as:  $(1/\xi)^{0.5}$  according to Seidel[12] i.e. a direct relation between damping and loads. Thus, for the current analysis, the variation is based on a variation in loads which then represent a variation in damping. Various investigations [1, 13] have indicated load reductions of 5-20% for the tower and foundation based on modified damping – and in this investigation load reductions of 5%, 10%, 15% and 20% have been applied.

The base case design has been based on the values given in Table 9.10. For the base case, the cost split of the turbine components (Figure 9.4), the CAPEX (Figure 9.2) and the full cost split (Figure 9.) are illustrated below.

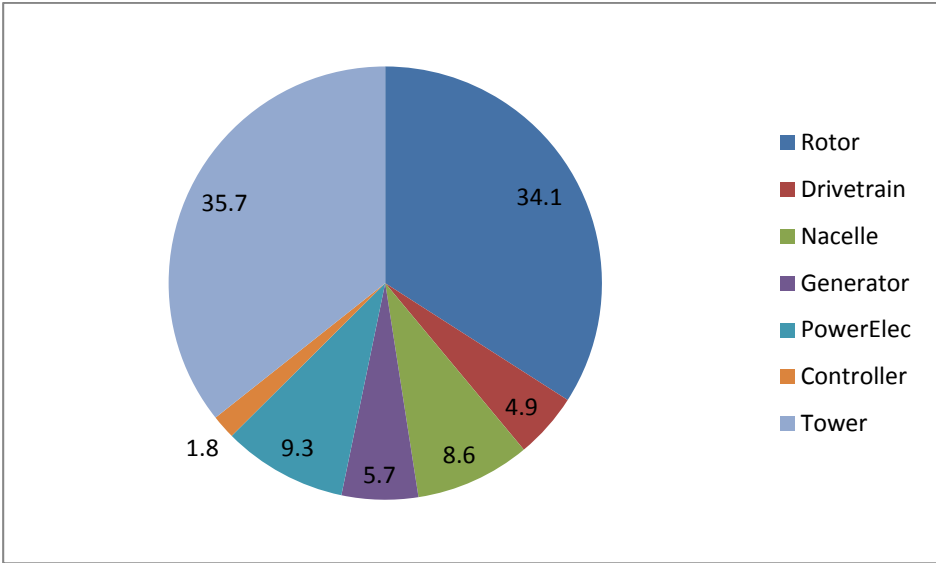


Figure 9.4 Turbine component cost split (Label values are percentage of the turbine total costs)

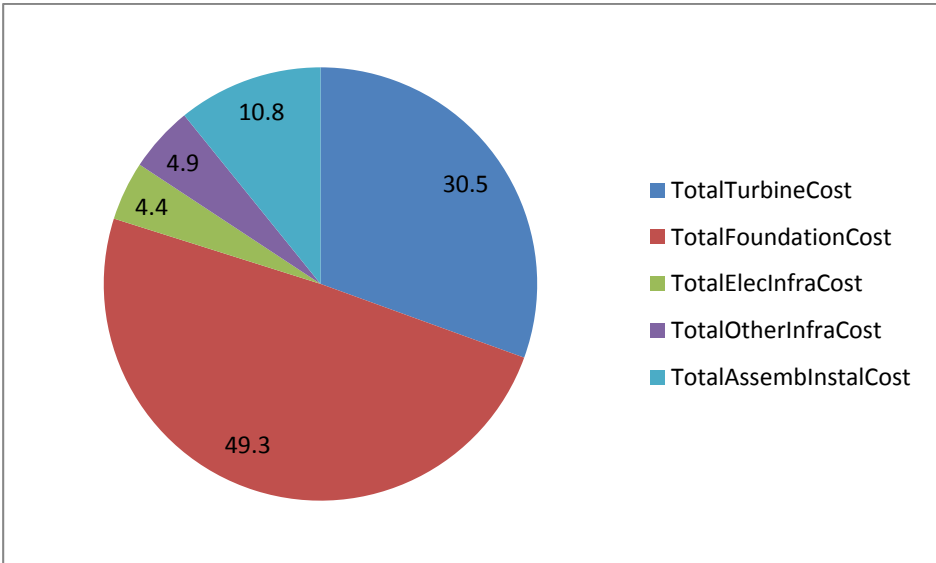


Figure 9.2 CAPEX cost split (Label values are percentage of the total CAPEX)

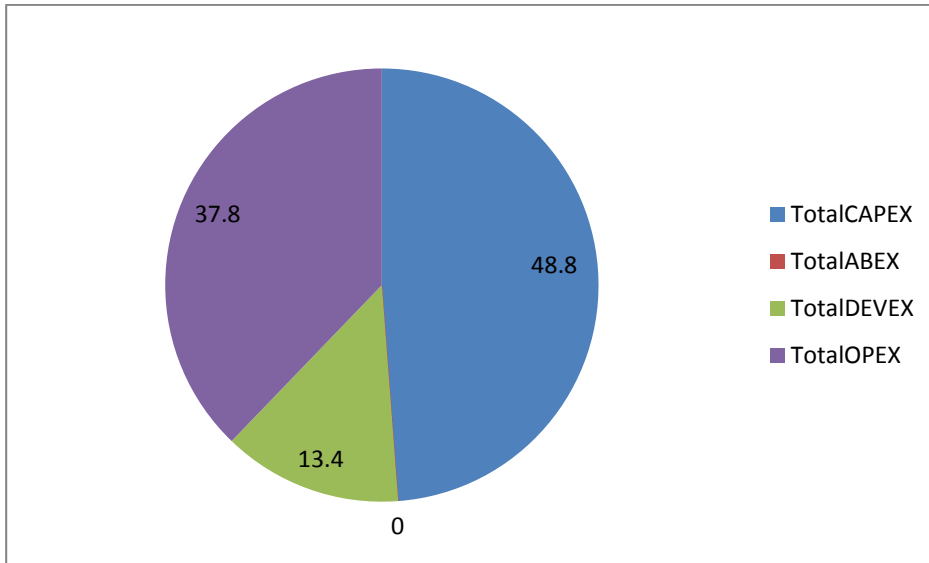


Figure 9.3 Full cost split (Label values are percentage of the total cost)

The outcome of the analysis is given in Table 9.11, Table 9.12 and Table 9.13.

The total cost of the turbine and the foundation is reduced when the design loads for these components are reduced, as expected. Note that only the total turbine cost is given in Table 9.11 and of this only the tower cost changes since no other component costs are a function of the tower loads. Since the tower is the only element which changes cost of the turbine, the relative change in the turbine cost with reduced load is lower than the foundation cost reduction. I.e. at a load reduction of 20%, the turbine cost is reduced 8% while the foundation cost is reduced 19%.

Table 9.11 CAPEX cost split for the different analyses

	Base case		Load red. 5%		Load red. 10%		Load red. 15%		Load red. 20%	
	[Meuro]	[%]	[Meuro]	[%]	[Meuro]	[%]	[Meuro]	[%]	[Meuro]	[%]
<b>TotalTurbineCost</b>	2.23	30.5	2.19	30.9	2.15	31.3	2.11	31.8	2.07	32.0
<b>TotalFoundation Cost</b>	3.60	49.3	3.42	48.3	3.24	47.2	3.05	46.2	2.92	45.2
<b>TotalElecInfraCost</b>	0.32	4.4	0.32	4.5	0.32	4.7	0.32	4.8	0.32	5.0
<b>TotalOtherInfraCost</b>	0.36	4.9	0.36	5.1	0.36	5.3	0.36	5.4	0.36	5.6
<b>TotalAssembInstallCost</b>	0.79	10.8	0.79	11.2	0.79	11.6	0.79	11.9	0.79	12.3
<b>TotalCAPEX</b>	7.30	100	7.08	100	6.86	100	6.63	100	6.46	100

The influence on the cost distribution is presented in Table 9.12 and the main results are given in Table 9.13. The base line LCOE is approximately 70 €/MWh and for a load reduction of 20%, this is reduced with 7% to a value of 65.5 €/MWh. These absolute numbers depends significantly on the assumed cost model parameters, while the relative change in LCOE is considered more robust.

The conclusion is that load reductions due to increased damping will have a significant impact on the component cost for the tower and the foundation, and the consequence for the levelized cost of energy is a significant reduction, too.

**Table 9.12 Full cost split for the different analyses**

	Base case		Load red. 5%		Load red. 10%		Load red. 15%		Load red. 20%	
	[Meuro ]	[%]	[Meuro ]	[%]	[Meuro ]	[%]	[Meuro ]	[%]	[Meuro ]	[%]
<b>TotalCAPE X</b>	7.30	48.8	7.08	48.10	6.86	47.3	6.63	46.5	6.46	45.8
		0				0		0		0
<b>TotalABEX</b>	0.00	0.00	0.00	0.00	0.00	0.00	0.00	0.00	0.00	0.00
<b>TotalDEVE X</b>	2.00	13.4	2.00	13.60	2.00	13.8	2.00	14.0	2.00	14.2
		0				0		0		0
<b>TotalOPEX</b>	5.65	37.8	5.65	38.30	5.65	38.9	5.65	39.5	5.65	40.0
		0				0		0		0
<b>Total cost</b>	14.95	100	14.73	100	14.51	100	14.28	100	14.11	100

**Table 9.13 Main results for the different analyses**

			Base case	Load red. 5%	Load red. 10%	Load red. 15%	Load red. 20%
<b>Total AEP incl. loss:</b>		[GWh]	282.27	282.27	282.27	282.27	282.27
<b>Total cost:</b>		[Meuro]	14.95	14.72	14.50	14.28	14.10
<b>Total discounted AEP:</b>		[GWh]	186.05	186.05	186.05	186.05	186.05
<b>Total discounted cost:</b>		[Meuro]	13.02	12.80	12.58	12.35	12.18
<b>LCOE:</b>		[Euro/MWh ]	69.99	68.79	67.60	66.40	65.46



## 10.0 Recommendations to IEC Standards

Based on the findings in the project as described in the preceding chapters, the following recommendations can be made to the IEC 61400-3 standard.

- The net damping of the support structure for monopiles is of the order of 1% critical without considering aerodynamics and without artificial tower damping.
- Mean site specific wind/wave misalignment of 10 Degs can be expected.
- The load reduction potential from increased support structure damping must be quantified by using measured wind and wave misalignment and measured directions of wind and wave impact around the support structure. There is little benefit of added support structure damping, if the predominant design driving load is the fore-aft moment, since this is driven by wind loads. On the other hand if the side-side moment is pre-dominant for any load case such as under storm conditions or under wind/wave misalignment, then benefit from higher support structure damping may be seen.
- It is common to observe nonlinear waves at water depths between 25m to 30m where the wave crests are much higher than the shallowness of wave troughs. Such nonlinear waves can occur even at small significant wave heights. The modeling of these waves requires at least second order irregular nonlinear methods, but higher order nonlinear models are preferred.
- The frequency of high mean wind speeds near cut-out can be higher than obtained using site specific annual probability distribution functions. It is therefore recommended to use a Rayleigh distribution which provides greater probability of high mean wind speeds near cut-out rather than site specific annual mean wind speed distributions with higher Weibull exponents.
- The contemporaneous loads and extrapolation of measured extreme loads on the blade root was done [14], whereby it was determined that instead of extrapolating a primary moment (ex. Flap moment and choosing a corresponding contemporaneous moment (ex. Edge moment), it was robust to extrapolate the blade root resultant moment. The blade root resultant moment was found to be less sensitive to outliers and the one year extreme was consistently within 10% of the absolute maximum sampled for the purpose of extrapolation.

## 11.0 Summary of Results and Dissemination

A complete instrumentation setup was installed on a 3.6 MW offshore wind turbine which included strain gauges, accelerometers, nacelle based LIDAR, anemometer and wave buoy at the foot of the turbine so as to validate the simulated loads. Dedicated databases to collect high frequency SCADA, wind, and wave and loads measurements have been made which were regularly storing the measurements.

The validation of extreme loads and fatigue loads based on load simulations in the HAWC2 software was completed. The main finding was the dependence of the loads on the damping of the support structure, which has been estimated based on measured tower accelerations. The investigation of the collected load measurements assessed the effect of wind/wave misalignment, extreme and fatigue loads, frequent storms and shutdowns of the wind turbines. The findings were published in three conference papers, two journal papers and a Ph.D. thesis.

A method for the reduction of uncertainties in design loads of the sub structure was determined based on quantifying the damping of the sub structure and by measuring the wave and wind joint distribution, by which Monte Carlo simulations can be run using the validated aeroelastic loads simulation code HAWC2. This will allow the user to appropriately determine the right percentile of design loads from the simulation results aligned to the targeted reliability level of the support structure. This can in turn lead to reduced downtime due to the ability to predict fatigue damage with lower O&M costs and allow site specific optimization for future installations. The implementation of the project recommendations as given in the previous chapter can lead to a reduction of the current support structure CAPEX in the order of 3-4%, based on the loads reduction potential achieved.

**References, List of Publications, Reports (Publications made from project results are in bold)**

- [1]. Koukoura, C., *Validated Loads Prediction Models for Offshore Wind Turbines for Enhanced Component Reliability*, Ph.D. Thesis, DTU Wind Energy, September 2014
- [2]. Koukoura, C., Natarajan, A., Krogh, T. and Kristensen, O.J., “Offshore Wind Turbine Foundation Model Validation with Wind Farm Measurements and Uncertainty Quantification”, *Proceedings of the Twenty-third (2013) International Offshore and Polar Engineering (ISOPE), Anchorage, June 2013*
- [3]. DNV-OS-J101, *Design of Offshore Wind Turbine Structures*, Det Norske Veritas, Hovik, Norway, 2007
- [4]. IEC 61400-1. *International Electrotechnical Committee, IEC 61400-1: Wind Turbines Part 1: Design Requirements*, Geneva, 2005
- [5]. IEC 61400-3. *International Electrotechnical Committee IEC 61400-3: Wind Turbines Part 3: Design Requirements for Offshore Wind Turbines*, Geneva, 2009
- [6]. Natarajan, A., “Influence of Second-Order Random Wave Kinematics on the Design Loads of Offshore Wind Turbine Support Structures”, *Renewable Energy Journal*, Vol. 68, 2014, pp. 829-841.
- [7]. Koukoura, C., Natarajan, A., Vesth, A., “‘Identification of support structure damping of a full scale offshore wind turbine in normal operation’ *Renewable Energy*, vol 81, pp. 882-895, 2015.
- [8]. Natarajan, A & Buhl, T, 'Reliability of Offshore Wind Turbine Drivetrains based on Measured Shut-down Events'. in *Proceedings of the Twenty-fifth (2015) International Ocean and Polar Engineering Conference*. International Society of Offshore and Polar Engineers, pp. 677-683, 2015.
- [9]. N. J. Tarp-Johansen, L. Andersen, C. E. D., C. Morch, B. Kallesoe, S. Frandsen, Comparing Sources of Damping of Cross-Wind Motion, in: *European Wind Energy Conference EWEC*, Stockholm, Sweden, 2009.
- [10]. M. Damgaard, J. K. Andersen, L. B. Ibsen, L. V. Andersen, Natural frequency and damping estimation of an offshore wind turbine structure, in *International Offshore and Polar Engineering Conference, ISOPE, Rhodes, Greece, 2012*.
- [11]. Shirzadeh R, Devriendt C, Bidakhvidi MA, Guillame P., “Experimental and computational damping estimation of an offshore wind turbine on a monopile foundation”, *Journal of Wind Engineering and Industrial Aerodynamics*, Vol. 120, 96-106, 2013
- [12]. Seidel, M. “Wave induced fatigue loads – Insights from frequency domain calculations” *Stahlbau* Vol. 83, Issue 8, 2013.
- [13]. Fischer, T.A. “Load Mitigation of an Offshore Wind Turbine by Optimization of Aerodynamic Damping and Vibration Control”, M. Sc. Thesis, Technical University of Denmark, July 2006
- [14]. Natarajan, A., Vesth, A and Lamata, R., “Extreme Design Loads Calibration of Offshore Wind Turbine Blades through Real Time Measurements”, *Proceedings of EWEA 2014, European Wind Energy Association, 2014*.